

27. PETROLOGY AND GEOCHEMISTRY OF BASALTS FROM DEEP SEA DRILLING PROJECT LEG 54

R.K. Srivastava, Department of Geology, Rajasthan University, Udaipur, India
and

R. Emmermann and H. Puchelt, Institut für Petrographie und Geochemie,
Universität Karlsruhe, Karlsruhe, Federal Republic of Germany

ABSTRACT

A suite of 89 basalt samples recovered at nine sites on DSDP Leg 54 from the East Pacific Rise (EPR) and Galapagos Rift (GR) have been analyzed for major oxides and trace elements. Basalts erupted at the EPR crest near 9°N, north of the Siqueiros fracture zone, are high-Fe and Ti tholeiites, whereas basalts ponded near an east-west trending ridge in the area are similar to more typical less fractionated ocean-floor basalts. The most fractionated EPR basalts with highest Fe and Ti are from the Siqueiros fracture zone.

The GR basalts range in chemistry from normal mid-ocean tholeiite to Fe- and Ti-enriched tholeiite. Both EPR and GR basalts are LIL-element and LREE-depleted. Galapagos Rift basalts have remarkably low concentrations of REE, K₂O, Sr, and Zr and appear to have been formed from a source material that has undergone greater partial melting than that encountered by EPR basalts.

There is a remarkable positive correlation between the element pairs Ti-Zr and Ti-Y for all sites. These, and variations in MgO, CaO, alkalis, Al₂O₃, Fe₂O, and TiO₂, are consistent with the basalts having experienced variable and, in some cases, extensive fractional crystallization from LIL-depleted melts. The dominating phases were plagioclase and clinopyroxene with lesser olivine. Basalts from many of the sites, notably GR basalts from Site 424, and Siqueiros fracture zone basalts, are more fractionated than typical Mid-Atlantic Ridge basalts.

INTRODUCTION

This paper presents petrographic and chemical data on 89 basalt samples from six sites on young East Pacific Rise (EPR) crust near 9°N, one site in the Siqueiros fracture zone (SFZ), and two sites from the flanks of the Galapagos Rift (GR), drilled during Leg 54 of the Deep Sea Drilling Project. The purpose of this study was (1) to characterize chemically and petrographically basalts from oceanic crust at the drilling sites of Leg 54, (2) to investigate the differences, if any, between the EPR, SFZ, and GR basalts, (3) to study the spatial variation amongst EPR basalts as a function of their distance from the EPR, (4) to determine the relationship, if any, between the rate of spreading and the nature of basalts, and finally (5) to evaluate the role of petrogenetic processes in the development of these basalts. Site locations and prominent sea-floor physiographic features mentioned in the text are shown on Figure 1. In this study, we distinguish sites drilled on abyssal hill topography on the flanks of the EPR (normal fabric topography) from those drilled in ponds in the moat-like structure adjacent to the OCP Ridge (Figure 1) and in the SFZ.

All 89 samples were renumbered in our laboratory. Table 1 lists our number and corresponding DSDP sample designation. For the sake of brevity, our numbers will be used throughout this report. The samples were thoroughly cleaned and submerged in double-distilled water for 24 hours. They were then dried at 60°C, and pulverized in an agate mill. The major oxide data were obtained by a combined atomic absorption and spectrophotometric scheme, as described by Srivastava (1977). FeO was measured titrimetrically by the classical dichromate method. H₂O was determined by the modified Penfield method. Ni, Cu, Zn, Y, Sr, Zr, and Rb were obtained by X-ray fluorescence analysis (XRF) on powder discs prepared by mixing in with a few drops of 2 per cent Moviol solution. A large number of International reference samples were used as standards (Flanagan, 1973). Rare earth elements Sc, Hf, Cr, and Co were determined in selected samples by instrumental neutron activation analysis (INAA), following the method of Puchelt and Kramar (1974).

Major oxide analyses for all 89 samples along with their C.I.P.W. norm are given in Table 2. Table 3 shows the trace element contents for the same samples and also

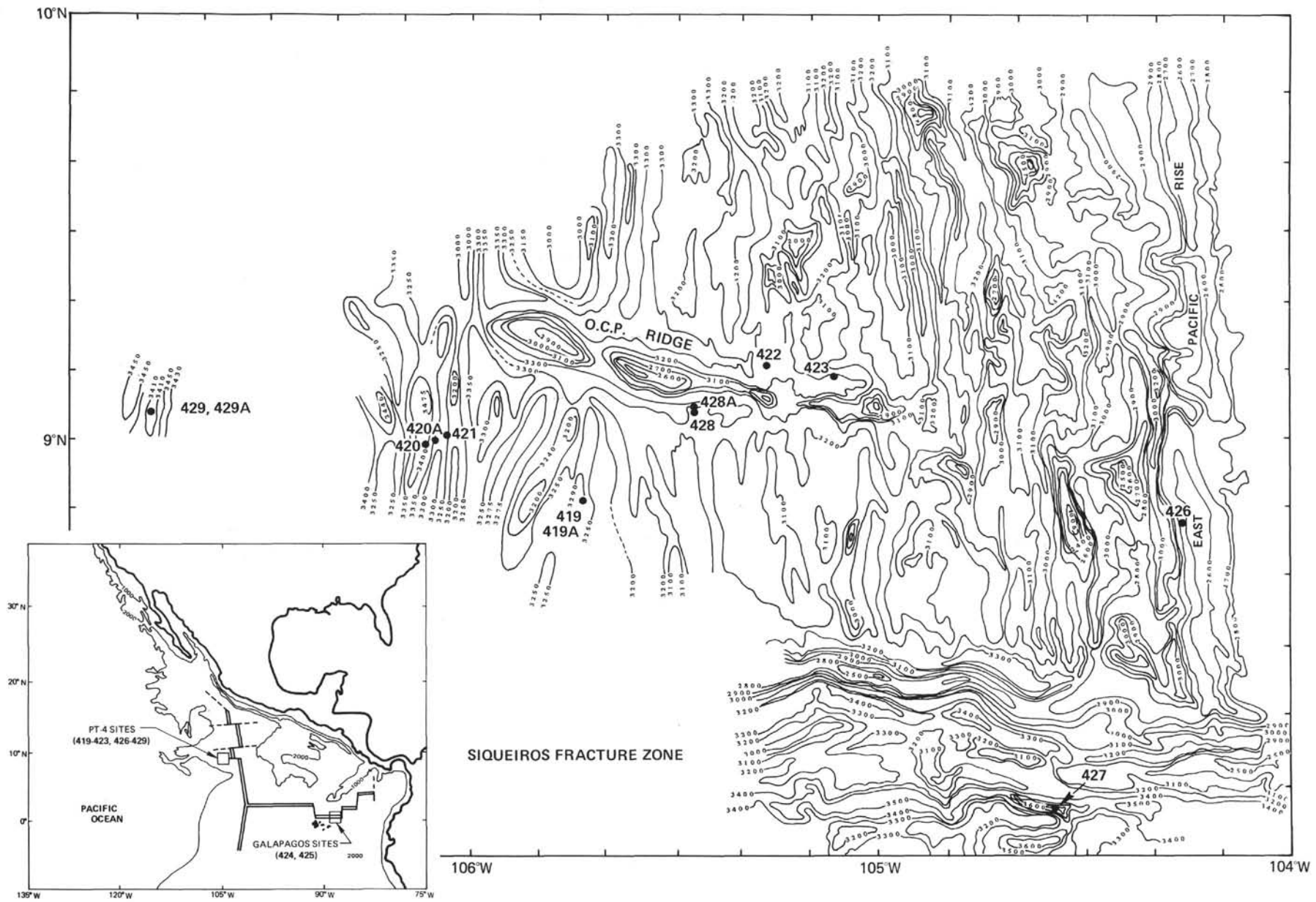


Figure 1. Location of sites drilled on DSDP Leg 54.

TABLE 1
Correlation of Our Sample and DSDP Sample Designations
for the Samples of this Study

Our Sample Designation	DSDP Sample Designation (Hole-Core-Section-Piece)	Our Sample Designation	DSDP Sample Designation (Hole-Core-Section-Piece)
RK 201	420-13, CC 1	RK 246	424B-6-1, 2
202	420-13, CC 4	247	424B-6-1, 9
203	420-14-1, 4	248	424B-6-1, 16
204	420-15-1, 6	249	424C-2-1, 3
205	420-17-1, 1	250	424C-3-1, 4
206	421-2-1, 1	251	425-7-1, 6
207	421-3-1, 4	252	425-7-1, 13
208	421-3-1, 16	253	425-7-1, 17a
209	421-3-1, 20	254	425-7-2, 7b
210	421-3-2, 2	255	425-7-2, 10
211	421-4-1, 5	256	425-8-1, 6
212	421-Bit, 3	257	425-8-1, 11
213	422-7-1, 6c	258	425-8-1, 16
214	422-7-1, 13	259	425-9-1, 11
215	422-8-5, 3	260	425-9-1, 14
216	422-9-1, 4d	261	425-9-1, 18
217	422-9-2, 5c	262	425-9-2, 3
218	422-9-3, 6a	263	425-9-2, 13
219	422-9-4, 13a	264	425-9-3, 10
220	422-9-5, 2	265	427-9-1, 2
221	422-10-1, 3	266	427-9-3, 6
222	423-5, CC 4	267	427-9-5, 7
223	423-6-1, 4	268	427-10-3, 4b
224	423-7-1, 7	269	428-5-4, 1
225	423-8-1, 1	270	428-6-1, 4
226	423-8-1, 7	271	428-6-2, 7
227	424-4-6, 4	272	428A-1-1, 1
228	424-5-1, 1	273	428A-1-1, 15
229	424-5-1, 8	274	428A-1-2, 7
230	424-5-1, 14a	275	428A-1-2, 10
231	424-5-2, 1c	276	428A-1-2, 12
232	424-5-3, 1	277	428A-1-3, 4
233	424-5-3, 9	278	428A-1-4, 7
234	424-5-4, 3	279	428A-2-1, 10
235	424-6-1, 2	280	428A-3-1, 6
236	424-6-1, 7	281	428A-3-1, 10b
237	424-6-1, 10b	282	428A-4-3, 4
238	424-6-2, 1b	283	428A-5-3, 11
239	424-6-3, 1c	284	428A-6-1, 11
240	424-7-1, 1	285	428A-7-2, 1a
241	424A-4-1, 2	286	429A-1-1, 2
242	424A-4-1, 6	287	429A-2-1, 3
243	424B-5-1, 8	288	429A-2-1, 14
244	424B-5-1, 12	289	429A-3-1, 4
245	424B-5-2, 2		

their FeO*/MgO and SI values.¹ The rare-earth and additional trace element data of some selected samples are given in Table 4. Tables 5a and b show the average composition of the magmas found at the EPR, SFZ, and GR sites.

Petrographic Summary of Basalts from the West Flank of the EPR—Holes 420, 421, 422, 423, 428, 428A, and 429A

Salient petrographic features of the basalts from the different holes are given in the appendix. We here summarize these features:

1) Basalts from Holes 420, 421, bottom of Holes 422, 423, and from the lower part of Hole 429A, are essentially glassy-cryptocrystalline to fine-grained aphyric to sparsely microphyric plagioclase-pyroxene basalts.

2) Depending upon the degree of crystallinity, the groundmass shows various textures such as hyalopilitic, spherulitic, variolitic, intersertal, and subophitic.

3) The glass present in these rocks is generally fresh. In some of the glassy basalts, the glass shows zonation;

¹ FeO* expresses total iron.

that is, (i) an outer light yellowish glass zone, (ii) a globular intermediate zone, and (iii) an aphanitic inner zone. This gradual textural variation is typical of pillow lavas.

4) In general the basalts are finely vesicular; the vesicles are either empty or filled with smectites.

5) At Holes 422, 428, 428A, and in the upper part of Hole 429A, there are two types of basaltic rocks: a fine-grained olivine-bearing basalt, and a fine- to medium-grained doleritic rock. The former is found at Hole 428 and the upper part of Holes 428A and 429A; the latter is found at Hole 422 and in the lower part of Hole 428A.

6) The olivine-bearing basalts from these holes are similar to the aphyric plagioclase-pyroxene basalts, except that the latter do not contain olivine. The amount of olivine in these rocks does not exceed one to two per cent.

7) At Hole 429A, the olivine-bearing basalts are younger than the magnetic anomaly age for the site, and they may not therefore have formed at the EPR proper.

8) The doleritic rocks at Holes 422 and 428A are mesocratic, fine- to medium-grained, and almost holocrystalline rocks, showing subophitic to ophitic texture. The chief mineral constituents are plagioclase, clinopyroxene, and titanomagnetite.

9) On the basis of the petrographic studies it can be concluded that the nature of basalts ponded near the OCP Ridge (Figure 1) — that is, basalts from Holes 422, 428, and 428A — is entirely different from that of the normal fabric basalt, that is, basalts from Holes 420, 421, 423, and the lower part of Hole 429A. Primarily, they are coarse-grained and apparently represented thick flows, sills, or even former lava lakes.

Petrographic Summary of Basalts from the SFZ

Petrographically, the basalts from Hole 427 are akin to the doleritic rocks from Holes 422 and 428A, except that they do not contain olivine which is occasionally present in the doleritic rocks. Furthermore, clinopyroxene microphenocrysts are much more common in these rocks, indicating that these have crystallized when the magma composition had left the olivine-plagioclase-pyroxene cotectic.

Petrographic Summary of Basalts from the GR—Holes 424, A, B, and C, and Hole 425

1) Megascopically, the basalts recovered from these holes can be described as fine- to medium-grained, vesicular aphyric basalts with occasional microphenocrysts of plagioclase. Microscopically, they show various textures. The quenched samples show hyalopilitic, variolitic, and intersertal texture, while relatively coarser samples show intergranular texture.

2) There are no significant petrographic differences in basalts from Holes 424, A, B, and C.

3) The minerals constituting these basalts are plagioclase, clinopyroxene, titanomagnetite, and variable amounts of glass.

4) Contrary to Site 424 basalts, the basalts from Hole 425 show large variation in their color, grain size, vesiculation, and mineral assemblages.

TABLE 2
Chemical Analyses and C.I.P.W. Norm of Basaltic Rocks, Leg 54

Site/Hole	420					421							422		
Sample	RK201	202	203	204	205	206	207	208	209	210	211	212	213	214	215
SiO ₂	50.73	50.96	51.25	50.24	50.01	50.25	49.69	51.25	51.07	51.39	51.50	50.25	50.25	50.55	50.55
TiO ₂	1.91	1.91	2.05	1.91	1.87	2.68	2.58	2.13	2.21	2.12	2.18	2.00	1.52	1.63	1.57
Al ₂ O ₃	14.31	13.91	14.25	14.54	13.90	13.70	13.32	13.17	13.12	13.00	13.12	13.43	14.25	14.00	13.93
Fe ₂ O ₃	4.96	4.93	4.95	5.23	4.54	6.42	6.82	5.40	6.01	6.80	5.21	6.99	3.55	3.49	4.09
FeO	6.20	6.50	5.15	5.55	7.85	6.60	6.60	5.50	5.25	4.75	6.00	5.65	6.70	6.75	6.20
MnO	0.18	0.18	0.19	0.19	0.19	0.22	0.21	0.20	0.21	0.19	0.22	0.21	0.18	0.19	0.19
MgO	6.42	6.52	6.63	6.65	7.00	6.01	5.95	6.52	6.63	6.47	6.56	6.87	8.02	7.90	7.90
CaO	11.01	10.95	11.21	10.95	11.21	9.94	9.87	11.01	11.40	10.66	10.73	10.73	11.68	11.53	11.53
Na ₂ O	2.55	2.43	2.56	2.59	2.52	2.66	2.55	2.66	2.63	2.55	2.66	2.60	2.69	2.69	2.72
K ₂ O	0.45	0.47	0.47	0.50	0.28	0.44	0.67	0.43	0.48	0.62	0.43	0.55	0.15	0.11	0.11
P ₂ O ₅ ⁺	0.15	0.16	0.12	0.13	0.16	0.19	0.20	0.17	0.16	0.17	0.19	0.16	0.13	0.15	0.13
H ₂ O	1.22	1.04	1.14	1.36	0.86	1.10	1.38	1.10	1.24	1.24	1.28	1.12	0.96	0.78	0.78
Total	100.09	99.96	99.87	99.84	100.39	100.21	99.75	99.54	100.41	99.97	100.08	100.56	100.08	99.77	99.70
C.I.P.W. Norm															
Q	1.37	2.09	2.06	0.39	—	2.09	1.25	2.35	1.41	2.62	2.69	—	—	—	—
or	2.70	2.82	2.83	3.01	1.66	2.64	4.04	2.59	2.88	3.73	2.58	3.29	0.90	0.66	0.66
ab	21.92	20.87	22.01	22.37	21.50	22.90	22.04	22.97	22.56	22.01	22.88	22.26	23.03	23.06	23.35
an	26.68	26.04	26.42	27.12	26.01	24.55	23.41	23.20	22.88	22.64	22.97	23.62	26.68	26.14	25.84
di	22.85	23.11	23.94	22.51	23.90	20.10	20.93	25.77	27.38	24.80	24.54	24.04	25.35	25.13	25.54
hy	18.20	18.89	16.63	18.58	19.51	19.77	20.35	16.58	16.20	17.67	17.61	19.23	14.27	17.74	17.01
ol	—	—	—	—	1.15	—	—	—	—	—	—	1.04	4.63	1.87	2.35
mt	2.06	2.12	1.86	2.00	2.30	2.40	2.49	2.01	2.06	2.11	2.06	2.31	1.90	1.90	1.91
il	3.69	3.68	3.95	3.71	3.58	5.18	5.00	4.13	4.26	4.11	4.21	3.84	2.92	3.14	3.02
ap	0.36	0.36	0.29	0.31	0.37	0.45	0.47	0.40	0.37	0.40	0.45	0.37	0.30	0.35	0.30

TABLE 2 — Continued

Site/Hole	424										424A		424B		
Sample	232	233	234	235	236	237	238	239	240	241	242	243	244	245	
SiO ₂	50.74	50.25	50.10	50.64	50.64	50.80	51.40	51.85	52.00	51.85	51.85	50.63	50.80	51.18	
TiO ₂	1.74	1.83	1.78	1.78	1.76	1.78	1.83	1.77	1.77	1.82	1.71	1.70	1.85	1.74	
Al ₂ O ₃	12.89	13.18	13.18	12.74	13.18	13.33	12.48	12.56	12.71	12.78	12.88	12.94	13.11	13.31	
Fe ₂ O ₃	4.05	4.42	2.76	2.72	2.82	2.45	3.09	3.00	3.10	2.22	2.42	3.27	3.60	2.61	
FeO	9.10	8.80	10.30	10.35	10.25	10.60	10.00	10.10	10.00	10.80	10.60	9.85	9.50	10.45	
MnO	0.21	0.20	0.21	0.21	0.22	0.20	0.20	0.20	0.22	0.23	0.21	0.20	0.20	0.20	
MgO	6.25	6.48	6.70	6.70	6.48	6.15	6.36	6.36	6.08	5.92	6.03	6.03	6.15	6.63	
CaO	10.19	10.50	10.50	10.30	10.19	10.20	10.71	10.51	10.71	10.71	10.33	10.14	9.95	9.58	
Na ₂ O	2.33	2.24	2.33	2.51	2.46	2.37	2.37	2.44	2.25	2.31	2.37	2.44	2.44	2.37	
K ₂ O	0.11	0.06	0.06	0.06	0.08	0.05	0.05	0.05	0.16	0.10	0.12	0.06	0.09	0.03	
P ₂ O ₅ ⁺	0.15	0.17	0.16	0.17	0.18	0.16	0.19	0.20	0.16	0.20	0.17	0.17	0.19	0.20	
H ₂ O	1.04	0.76	0.90	0.84	0.72	1.38	1.26	1.24	1.14	1.44	1.54	1.96	1.86	0.88	
Total	98.80	98.89	98.98	99.02	98.98	99.47	99.94	100.30	100.30	100.38	100.19	99.39	99.74	99.18	
C.I.P.W. Norm															
Q	4.02	3.32	2.32	2.48	2.86	3.97	4.26	4.50	5.26	5.30	5.03	3.87	4.03	4.39	
or	0.66	0.36	0.36	0.36	0.48	0.31	0.30	0.30	0.96	0.60	0.72	0.36	0.54	0.18	
ab	20.24	19.39	20.15	21.68	21.22	20.49	20.37	20.90	19.25	19.79	20.35	21.25	21.16	20.45	
an	25.03	26.32	25.88	23.81	25.17	26.13	23.63	23.45	24.27	24.51	24.51	24.88	25.15	26.08	
di	21.43	21.39	21.74	22.52	20.84	20.31	24.08	23.20	23.48	23.22	21.90	21.37	20.03	17.40	
hy	22.37	22.77	23.34	22.82	23.03	22.48	20.89	21.81	20.46	20.15	21.31	22.02	22.54	25.17	
ol	—	—	—	—	—	—	—	—	—	—	—	—	—	—	
mt	2.48	2.50	2.47	2.49	2.49	2.49	2.48	2.47	2.45	2.45	2.48	2.51	2.48	2.49	
il	3.39	3.56	3.45	3.45	3.47	3.45	3.53	3.40	3.40	3.50	3.20	3.32	3.60	3.36	
ap	0.36	0.40	0.38	0.40	0.43	0.38	0.45	0.47	0.37	0.47	0.40	0.40	0.45	0.47	

5) Three to four distinct petrographic types, namely (i) aphyric to sparsely phyrlic plagioclase-pyroxene basalts, (ii) phyrlic-glomeroporphyritic basalts, (iii) glomeroporphyritic ± olivine, (iv) plagioclase-pyroxene ± olivine sparsely phyrlic basalts, constitute the entire column drilled at Hole 425.

CHEMISTRY OF BASALTS

The major, minor and trace element data of 89 samples are given in Tables 2, 3, and 4. Before attempting to classify and interpret the mode of origin of these basalts, it would be useful to discuss the salient

TABLE 2 – Continued

422						423					424				
216	217	218	219	220	221	222	223	224	225	226	227	228	229	230	231
49.70	49.33	49.36	49.08	49.27	50.27	50.57	51.00	51.68	49.53	49.94	50.44	50.35	51.10	51.10	50.79
1.59	1.39	1.50	1.30	1.43	2.03	2.13	2.14	2.21	2.02	2.04	1.87	1.85	1.81	1.82	1.81
14.18	15.35	15.06	15.84	15.28	13.65	13.75	13.54	13.34	13.69	13.77	12.86	12.83	12.82	12.96	12.96
3.64	3.74	3.87	3.54	3.01	2.94	4.75	5.16	5.00	6.16	5.70	2.88	3.00	2.98	3.10	3.33
6.70	5.45	5.40	4.80	6.10	8.00	6.60	6.60	7.20	6.20	6.20	10.20	10.10	10.10	10.00	9.80
0.18	0.20	0.18	0.30	0.17	0.20	0.22	0.20	0.19	0.19	0.19	0.21	0.21	0.21	0.21	0.21
7.74	8.22	8.56	8.06	8.56	7.25	6.63	6.73	6.33	6.48	6.04	6.48	6.50	6.48	6.63	6.55
11.53	11.53	11.53	12.03	11.78	11.28	10.17	10.55	10.31	10.41	10.41	10.29	10.29	10.19	10.29	10.19
2.72	2.80	2.72	2.78	2.72	2.63	2.70	2.69	2.69	2.74	2.89	2.48	2.48	2.48	2.55	2.28
0.10	0.19	0.21	0.17	0.21	0.31	0.35	0.38	0.38	0.40	0.32	0.08	0.18	0.11	0.11	0.10
0.12	0.15	0.15	0.13	0.13	0.17	0.25	0.20	0.20	0.19	0.21	0.18	0.18	0.20	0.18	0.15
0.80	0.96	0.74	1.36	0.60	0.96	1.32	0.78	0.22	1.38	1.06	1.14	1.18	1.16	0.56	0.74
99.00	99.31	99.28	99.39	99.28	99.69	99.44	99.97	99.75	99.39	98.79	99.11	99.15	99.64	99.51	98.91
–	–	–	–	–	–	1.85	1.50	3.04	–	0.58	2.66	2.21	3.34	2.55	3.86
0.60	1.14	1.26	1.02	1.26	1.86	2.12	2.28	2.28	2.42	1.94	0.48	1.09	0.66	0.66	0.60
23.51	24.17	23.42	24.07	23.99	22.60	23.38	23.04	23.01	23.79	25.16	21.51	21.51	21.40	21.90	19.70
26.75	29.34	28.75	30.95	29.32	24.90	24.92	24.04	23.45	24.49	24.33	24.30	23.93	23.99	23.93	25.36
25.20	22.75	23.06	23.71	23.66	25.19	20.55	22.70	22.19	22.45	22.60	22.19	22.51	21.72	22.07	20.92
14.10	8.59	9.35	5.81	7.21	18.89	20.32	19.67	19.09	19.29	18.69	22.53	22.47	22.68	22.73	23.19
4.52	9.25	9.16	10.03	10.37	0.18	–	–	–	0.87	–	–	–	–	–	–
1.94	1.70	1.73	1.55	1.71	2.06	2.11	2.18	2.21	2.29	2.22	2.24	2.24	2.21	2.22	2.49
3.08	2.69	2.90	2.53	2.76	3.92	4.14	4.11	4.25	3.94	3.98	3.64	3.60	3.51	3.51	3.51
0.29	0.36	0.36	0.31	0.30	0.40	0.59	0.47	0.47	0.45	0.50	0.43	0.43	0.47	0.43	0.36

TABLE 2 – Continued

424B			424C		425										
246	247	248	249	250	251	252	253	254	255	256	257	258	259	260	261
51.33	51.18	51.18	50.99	50.84	50.90	51.18	51.18	51.00	49.93	50.38	50.23	50.53	50.53	50.69	50.58
1.73	1.80	1.74	1.84	1.91	1.34	1.36	1.31	1.09	1.14	1.24	1.02	0.90	0.96	0.92	0.97
13.47	13.33	13.75	12.80	12.86	13.75	13.80	13.80	14.20	14.35	13.92	14.86	13.91	14.20	14.28	14.80
2.67	2.68	3.10	2.28	1.98	3.26	2.77	2.72	3.55	3.85	3.47	3.14	2.86	3.18	4.67	3.47
10.40	10.35	10.00	10.75	10.90	8.90	9.20	8.90	7.70	7.60	7.50	7.15	7.10	7.30	6.75	7.60
0.21	0.21	0.20	0.23	0.23	0.19	0.19	0.19	0.17	0.18	0.16	0.16	0.15	0.17	0.17	0.18
6.39	6.63	6.63	6.63	6.63	7.67	7.52	8.00	8.16	8.00	8.16	8.30	8.50	8.42	8.16	8.42
9.95	10.14	10.25	10.83	10.56	11.43	11.43	11.52	11.95	12.17	11.75	12.17	12.17	12.00	11.75	11.95
2.31	2.31	2.31	2.31	2.27	2.20	2.14	2.00	2.00	1.87	1.87	1.73	1.61	1.87	1.73	1.75
0.16	0.16	0.16	0.16	0.10	0.08	0.05	0.03	tr.	0.05	0.05	0.03	0.03	0.03	0.18	0.03
0.17	0.20	0.20	0.16	0.16	0.12	0.12	0.12	0.08	0.12	0.12	0.08	0.12	0.12	0.08	0.08
0.98	0.90	0.90	0.60	0.80	0.76	0.74	0.74	0.74	0.44	0.86	0.74	1.36	0.46	0.60	0.70
99.77	99.89	100.42	99.58	99.24	100.60	100.50	100.51	100.64	99.70	99.48	99.61	99.24	99.24	99.97	100.53
4.20	3.63	3.23	2.99	3.63	1.19	2.13	2.26	2.19	0.60	1.94	1.54	2.92	1.43	1.76	1.32
0.96	0.96	0.96	0.96	0.60	0.47	0.30	0.18	–	0.30	0.31	0.18	0.18	0.18	1.07	0.18
19.83	19.78	19.69	19.78	19.54	18.70	18.19	16.99	17.16	15.99	16.08	14.84	13.95	16.06	14.79	14.86
26.28	25.84	26.87	24.38	25.03	27.53	28.03	28.71	30.19	30.95	29.93	33.15	31.37	30.71	30.98	32.56
18.78	19.65	19.06	23.94	22.49	23.56	23.15	22.88	23.98	24.12	23.34	22.48	24.17	23.61	22.44	21.61
23.74	23.75	23.94	21.57	22.18	23.45	23.10	24.02	22.08	23.48	23.66	23.72	23.49	23.91	24.89	25.28
–	–	–	–	–	–	–	–	–	–	–	–	–	–	–	–
2.48	2.45	2.46	2.47	2.45	2.26	2.23	2.17	2.10	2.12	2.05	1.93	1.88	1.96	2.11	2.14
3.34	3.46	3.32	3.53	3.69	2.55	2.59	2.50	2.10	2.19	2.38	1.97	1.75	1.85	1.77	1.84
0.40	0.47	0.46	0.37	0.38	0.28	0.28	0.28	0.19	0.23	0.28	0.19	0.29	0.28	0.19	0.15

features of their chemistry and to see if these could be related to the mineralogical variations encountered within these basalts.

Site 420

Five analyzed samples of basalts show very little or no chemical variation with respect to their major and trace element chemistry, which is in keeping with limited or no variation in petrography. Their relatively high

TiO₂ (1.87 to 2.05%), K₂O (about 0.5%, except for one sample which has 0.28%), Zr (154 to 164 ppm), and Rb (6 to 12 ppm), coupled with relatively high FeO/MgO, and low Al₂O₃ and Ni, imply that these rocks are highly fractionated.

Hole 421

Seven chemical analyses of basalts are given in Tables 2 and 3. The data reveal that there are two types or

TABLE 2 – Continued

Site/Hole	425			427				428			428A			
Sample	262	263	264	265	266	267	268	269	270	271	272	273	274	275
SiO ₂	50.45	49.80	50.55	49.95	50.40	49.55	50.30	49.50	50.10	50.10	49.80	50.05	50.20	49.95
TiO ₂	1.01	1.00	1.02	2.57	2.58	2.64	2.53	1.50	1.57	1.61	1.55	1.64	1.58	1.60
Al ₂ O ₃	14.52	14.06	14.21	13.75	13.75	13.75	13.91	14.52	14.45	14.83	14.83	15.05	14.67	15.28
Fe ₂ O ₃	3.64	3.77	3.53	3.95	3.41	4.16	4.38	3.38	4.81	3.87	3.61	4.06	3.32	2.91
FeO	7.35	7.20	7.40	8.70	9.40	9.00	8.40	7.05	6.05	6.60	6.50	6.40	7.20	7.30
MnO	0.17	0.17	0.17	0.23	0.20	0.20	0.18	0.18	0.18	0.20	0.20	0.26	0.21	0.20
MgO	8.00	8.35	8.43	6.35	6.63	6.63	6.80	7.66	7.31	7.48	7.58	7.48	7.66	7.29
CaO	11.61	11.89	12.00	9.94	9.57	9.83	9.73	11.89	11.45	11.72	11.72	11.89	11.72	11.85
Na ₂ O	2.12	2.17	2.20	3.06	3.06	2.88	2.88	2.65	2.65	2.50	2.65	2.65	2.65	2.50
K ₂ O	0.01	0.01	0.01	0.06	0.10	0.10	0.08	0.12	0.19	0.12	0.12	0.12	0.06	0.25
P ₂ O ₅ +	0.11	0.10	0.11	0.29	0.30	0.30	0.20	0.19	0.19	0.18	0.19	0.19	0.18	0.18
H ₂ O	0.90	0.86	0.60	1.00	0.98	1.08	1.06	0.42	0.30	1.06	0.56	0.86	0.64	0.88
Total	99.89	99.38	100.22	99.85	100.38	100.12	100.54	99.06	99.25	100.27	99.31	100.65	100.09	99.99
C.I.P.W. Norm														
Q	0.75	—	—	0.50	0.71	0.30	1.09	—	—	—	—	—	—	—
or	0.06	0.06	0.06	0.36	0.60	0.60	0.47	0.72	1.14	0.72	0.72	0.72	0.35	
ab	18.18	18.68	18.82	22.28	26.12	24.69	24.58	22.80	22.76	21.40	22.78	22.55	22.61	
an	30.48	29.12	29.08	23.96	23.70	24.62	25.00	27.83	27.38	29.21	28.67	28.98	28.19	
di	22.24	24.76	24.68	19.94	18.32	18.82	17.87	25.24	23.75	23.21	23.96	23.78	23.91	
hy	24.05	21.20	22.39	20.96	22.53	22.73	23.05	12.42	17.24	18.83	14.64	14.36	16.43	
ol	—	1.96	0.72	—	—	—	—	5.70	2.25	1.18	3.97	4.12	3.11	
mt	2.04	2.06	2.04	2.37	2.38	2.45	2.37	1.94	2.00	1.93	1.89	1.92	1.96	
il	1.94	1.94	1.96	4.95	4.94	5.08	4.85	2.90	3.03	3.09	2.97	3.13	3.02	
ap	0.25	0.23	0.25	0.68	0.71	0.71	0.71	0.45	0.45	0.42	0.38	0.44	0.42	

groups of basalts. Two samples from Core 2 and the upper part of Core 3 (RK 206 and 207) represent a magma type richer in TiO₂ and Zr, and poorer in Ca as compared with the remaining five basalts. The FeO*/MgO ratio in the group is also much higher than in the others.

These two distinct chemical types correspond with the two petrographic types encountered within the hole. The high TiO₂, Zr, and high FeO*/MgO type represents the glassy basalts, and the other group represents the aphyric to sparsely microphyric basalts.

Hole 422

The analyzed nine samples from this hole, except for one sample from the bottom, differ significantly from the basalts from Holes 420 and 421. All samples are significantly richer in MgO, and poorer in TiO₂ as compared with the basalts from Holes 420 and 421. Besides these differences in major oxides, there are also characteristic differences in trace elements. For example, Zr and Sr contents of these rocks range from 98 to 122 ppm and 136 to 172 ppm, respectively, whereas at Holes 420 and 421 the same elements vary from 154 to 212 ppm and 104 to 132 ppm, respectively.

The basalts from Hole 422 can be grouped into three distinct chemical groups, corresponding to three different petrographic units in the hole, namely the upper doleritic unit, the lower doleritic unit, and the aphyric basalt in the bottom of the hole. The chemical analyses in Table 4a reveal that the upper doleritic unit (magma group, Core 422-1) is richer in Ti and Fe and poorer in Mg, Ca, and Al than the lower doleritic unit (magma group, Core 422-2). Amongst the trace elements in these two groups also, there are significant differences, particularly in Ni, Sr, and Zr. These differences in the chemistry can be attributed to the presence of olivine

and larger numbers of plagioclase phenocrysts in the lower doleritic unit.

The third magma group at this hole (Core 422-3, Table 5a), represented by the single aphyric basalt found at the bottom of the hole below the doleritic rocks, is characterized by high Ti (TiO₂ = 2.03%), Zr (144 ppm), and FeO*/MgO (1.51), and low Al (Al₂O₃ = 13.65%), Sr (109 ppm), and Ni (65 ppm). It resembles closely the basalts from Holes 420 and 421.

Hole 423

Five analyzed samples of basalts from this hole are similar to basalts from Holes 420 and 421; that is, they are characterized by high Ti (TiO₂ = 2.02 to 2.22%) high FeO/MgO (1.63 to 1.86), and low Al (Al₂O₃ = 13.34 to 13.77%). Zr and Y in these basalts are also high. On the basis of their FeO*/MgO and SI (Solidification Index) values, they can be divided into two sub-groups. The analyses of these sub-groups given in Table 5a (Cores 423-1 and 2) reveal that there are no major differences between the two types, which is in keeping with the limited variation in the petrography of these basalts. The Core 423-1 type, found in the upper part of the hole, most likely represents a slightly less fractionated magma than that of Core 423-2.

Holes 428 and 428A

Chemical analyses of basalts from these holes are given in Tables 2, 3, and 4. There are no large-scale variations in the chemistry of these basalts. The aphyric olivine basalts from Hole 428 and the upper part of Hole 428A are similar to those of the doleritic unit in the lower part of Hole 428A, except that the MgO content of the doleritic unit and its SI values are slightly higher than those of the olivine basalts. Thus, the olivine

TABLE 2 – Continued

428A										429A			
276	277	278	279	280	281	282	283	284	285	286	287	288	289
50.00	49.88	50.83	51.23	51.53	50.58	51.08	50.38	50.58	50.38	49.88	49.98	50.63	50.48
1.53	1.51	1.62	1.54	1.56	1.56	1.53	1.48	1.50	1.55	1.15	1.19	1.62	1.62
16.00	14.91	14.84	15.05	14.84	14.53	14.24	15.06	14.45	14.31	16.19	15.82	14.31	14.38
2.22	2.43	2.47	4.23	3.88	3.44	3.07	2.95	2.70	2.94	2.97	3.80	4.35	3.28
7.70	7.05	7.80	6.00	5.60	6.80	7.30	7.20	7.20	7.20	5.20	5.20	7.45	7.80
0.20	0.19	0.19	0.17	0.17	0.16	0.17	0.17	0.15	0.17	0.14	0.13	0.19	0.18
7.00	7.44	7.35	7.00	7.29	7.59	8.09	7.97	7.91	7.91	7.29	7.29	7.22	7.15
11.85	11.44	11.04	11.05	11.25	11.04	11.04	11.44	11.44	11.04	12.25	12.05	10.65	11.04
2.63	2.56	2.56	2.63	2.63	2.50	2.50	2.52	2.52	2.50	2.50	2.43	2.50	2.50
0.24	0.24	0.25	0.24	0.25	0.17	0.14	0.18	0.16	0.16	0.08	0.14	0.32	0.26
0.19	0.19	0.19	0.19	0.21	0.20	0.18	0.20	0.19	0.19	0.13	0.13	0.20	0.19
0.78	0.76	0.80	0.84	0.64	0.80	0.88	0.66	0.80	0.94	1.32	1.12	0.52	0.60
100.34	99.60	99.94	100.18	99.70	99.37	100.22	100.18	99.60	99.29	99.10	99.28	99.96	99.45
—	—	0.60	1.16	1.45	0.78	0.64	—	—	0.28	—	—	0.46	0.58
1.43	1.44	1.50	1.43	1.50	1.02	0.84	1.07	0.96	0.97	0.48	0.85	1.91	1.56
22.40	21.98	21.89	22.48	22.51	21.53	21.35	21.47	21.65	21.57	21.70	21.01	21.35	21.46
31.33	28.90	28.56	28.87	28.26	28.41	27.46	29.46	27.97	27.88	33.55	32.55	27.13	27.65
21.73	22.43	20.88	20.67	21.83	21.23	21.72	21.51	23.05	21.75	22.66	22.56	20.45	21.86
13.97	16.90	21.10	20.09	19.21	21.65	22.70	18.89	21.14	22.21	16.26	18.02	22.94	21.28
3.92	3.03	—	—	—	—	—	2.42	0.02	—	1.28	0.71	—	—
1.85	1.96	1.92	1.89	1.75	1.91	1.93	1.88	1.86	1.90	1.52	1.67	2.18	2.06
2.93	2.90	3.11	2.95	2.99	2.99	2.94	2.83	2.89	2.99	2.24	2.30	3.11	3.12
0.44	0.45	0.44	0.44	0.50	0.47	0.42	0.46	0.45	0.45	0.30	0.30	0.46	0.45

TABLE 3
Trace Element Contents (ppm) and FeO*/MgO Ratio, Basaltic Rocks, Leg 54

Sample	Ni	Cu	Zn	Y	Sr	Zr	Rb	Li	FeO*/MgO	SI	Sample	Ni	Cu	Zn	Y	Sr	Zr	Rb	Li	FeO*/MgO	SI
RK 201	82	51	99	45	111	160	9	5	1.65	31.19	RK 246	56	57	110	38	65	106	2	—	1.98	29.14
202	69	60	96	44	108	154	12	6	1.67	31.27	247	56	70	92	45	68	113	1	—	1.91	29.96
203	93	59	105	39	121	161	6	5	1.44	33.55	248	49	52	83	45	66	115	1	—	1.91	29.86
204	74	52	94	45	120	164	12	7	1.53	32.40	249	29	53	117	40	67	121	2	—	1.92	29.96
205	92	57	103	45	113	164	10	4	1.69	31.55	250	36	49	115	35	59	126	2	—	1.90	30.30
206	63	54	104	53	126	212	tr	5	2.05	27.16	251	56	64	96	30	57	77	1	3	1.53	34.69
207	49	50	96	48	114	197	4	5	2.13	26.34	252	47	61	94	29	55	82	1	2	1.54	34.69
208	62	64	99	51	128	179	8	7	1.58	31.79	253	50	63	81	30	55	74	1	2	1.41	36.95
209	69	65	99	49	126	171	6	6	1.60	31.57	254	59	68	74	24	57	71	1	2	1.33	38.11
210	75	86	96	47	132	168	12	6	1.67	30.53	255	70	74	75	27	52	61	1	1	1.37	37.44
211	98	50	109	49	130	184	3	5	1.62	31.45	256	62	68	71	24	54	62	1	1	1.29	38.76
212	56	58	85	43	104	185	4	6	1.73	30.32	257	62	72	73	24	54	50	1	1	1.19	40.79
213	66	55	74	29	140	122	1	5	1.23	37.99	258	70	68	68	16	62	41	1	1	1.13	42.08
214	67	58	85	34	148	119	1	7	1.24	37.73	259	70	72	80	19	49	48	1	1	1.20	40.48
215	41	48	70	35	136	116	1	6	1.24	37.58	260	70	79	95	25	52	45	1	1	1.33	37.97
216	50	46	68	24	142	100	1	5	1.28	37.03	261	56	71	75	25	57	49	1	2	1.27	39.58
217	114	59	72	28	182	108	1	5	1.07	40.29	262	56	74	85	27	60	50	1	2	1.32	37.88
218	122	50	58	24	167	102	1	7	1.04	41.23	263	99	71	69	27	59	49	1	2	1.26	38.84
219	107	55	72	25	176	98	1	7	0.99	41.65	264	65	72	79	24	54	45	1	2	1.25	39.08
220	103	52	61	20	172	105	1	5	1.02	41.55	265	46	50	82	46	130	190	1	—	1.92	28.71
221	65	53	65	31	109	144	1	6	1.46	34.31	266	50	46	94	45	124	186	1	—	1.87	29.33
222	63	59	104	37	122	160	1	7	1.63	31.52	267	62	50	86	46	120	193	1	—	1.91	29.11
223	56	45	90	40	122	155	1	6	1.66	31.22	268	52	46	82	42	110	194	1	—	1.80	30.17
224	47	60	98	46	125	163	1	6	1.77	29.31	269	62	69	78	26	128	99	3	—	1.31	36.72
225	47	55	98	43	132	164	1	4	1.80	29.48	270	69	77	78	24	124	103	4	—	1.41	34.79
226	52	59	98	46	130	160	1	1	1.86	28.56	271	70	64	74	29	128	107	2	—	1.34	36.36
227	44	53	87	39	62	132	1	6	1.96	29.29	272	69	60	74	27	130	102	2	—	1.28	37.05
228	38	61	103	38	68	121	1	6	1.95	29.20	273	66	72	82	27	128	107	1	—	1.34	36.11
229	44	55	103	38	66	129	1	8	1.96	29.26	274	59	63	70	29	130	101	1	—	1.32	36.67
230	66	59	98	37	65	116	1	6	1.91	29.61	275	65	60	66	28	136	94	2	—	1.35	36.00
231	44	48	82	36	66	109	2	5	1.94	29.69	276	74	67	70	21	128	94	2	—	1.37	35.37
232	49	59	98	39	65	114	1	8	2.02	28.62	277	56	62	68	27	139	98	1	—	1.35	35.91
233	44	55	94	37	64	116	1	9	1.96	29.45	278	62	52	64	28	128	97	1	—	1.35	35.98
234	50	59	98	38	60	110	1	8	1.89	30.24	279	67	59	66	21	131	120	2	—	1.39	34.83
235	40	55	94	35	64	110	2	8	1.89	29.99	280	80	59	72	30	145	100	1	—	1.24	37.10
236	49	54	117	38	68	125	1	5	1.96	29.33	281	62	53	70	29	145	96	1	—	1.30	37.02
237	52	61	115	37	68	123	1	6	2.07	28.44	282	68	60	72	26	136	99	2	—	1.23	38.34
238	56	88	107	40	68	130	1	6	1.99	29.08	283	75	79	71	24	125	101	2	—	1.23	38.28
239	49	55	103	38	68	129	1	5	2.00	28.97	284	69	66	62	25	131	97	2	—	1.24	38.60
240	52	61	110	40	66	130	3	5	2.08	28.16	285	59	67	63	26	139	95	1	—	1.24	38.19
241	54	65	109	40	71	128	3	5	2.14	27.73	286	140	76	73	20	139	64	1	—	1.07	40.41
242	49	61	113	43	65	131	2	6	2.10	27.99	287	138	74	62	22	136	66	1	—	1.17	38.65
243	56	66	115	40	71	125	1	—	2.11	27.85	288	89	48	82	32	115	100	3	—	1.57	33.06
244	59	57	107	35	61	115	2	—	2.07	28.24	289	86	53	82	29	114	106	4	—	1.49	34.06
245	46	61	98	40	68	123	1	—	1.92	30.01											

Notes: FeO* = total iron as FeO. SI = 100 MgO/MgO + Fe₂O₃ + FeO + Na₂O + K₂O.

TABLE 4
Rare-earth and Additional Trace Element Contents of Selected Samples, Leg 54

Sample	Na ₂ O	Fe ₂ O ₃	Sc	Cr	Co	Hf	La	Ce	Nd	Sm	Eu	Gd	Tb	Ho	Tm	Yb	Lu
RK 261	n.d.	10.97	47	267	47	<1	1.0	3.9	5.1	2.1	0.86	3.4	0.65	1.0	0.43	2.7	0.49
262	2.08	11.55	49	274	49	<1	1.2	3.8	5.5	2.2	0.91	3.2	0.65	0.97	0.47	2.7	0.43
263	2.12	10.89	43	254	46	<1	1.3	4.1	5.4	1.9	0.84	3.4	0.56	0.95	0.40	2.6	0.39
264	2.09	11.32	47	268	49	<1	0.99	3.6	5.1	2.1	0.88	3.2	0.61	0.96	0.43	2.8	0.44
265	3.21	13.40	43	97	44	4.5	7.1	18	15	5.8	2.2	6.6	1.3	1.8	0.93	5.1	0.74
266	3.00	13.96	42	106	43	4.4	7.0	16	18	5.8	2.1	6.5	1.4	2.0	0.87	4.9	0.69
267	2.92	14.01	41	90	42	5.4	6.6	16	16	5.6	1.9	6.8	1.4	1.8	0.78	4.6	0.72
268	3.09	14.29	44	110	46	4.7	7.0	17	15	5.8	2.1	6.9	1.4	2.3	0.77	5.0	0.75
269	2.77	10.32	40	304	40	2.5	3.8	12	9.0	3.4	1.26	4.3	0.85	1.1	0.50	2.8	0.53
270	2.66	9.94	39	282	39	1.3	4.9	11	9.5	3.4	1.35	4.3	0.77	1.2	0.52	2.8	0.42
271	2.70	10.26	41	275	41	3.3	4.0	10	11	3.5	1.33	5.5	0.70	1.0	0.58	2.8	0.46
272	2.83	10.03	41	305	41	2.7	4.3	10	11	3.5	1.40	4.5	0.87	1.1	0.49	3.2	0.49
273	2.61	9.76	39	268	40	2.6	4.0	10	9.6	3.4	1.34	4.1	0.75	1.3	0.59	2.8	0.48
274	2.77	10.36	41	287	41	1.6	4.0	10	9.5	3.6	1.32	4.0	0.84	1.3	0.53	3.0	0.45
275	2.70	10.01	41	301	41	1.4	4.3	10	9.8	3.5	1.36	4.2	0.95	1.4	0.54	3.0	0.48
276	2.75	9.63	41	314	41	2.5	3.9	11	9.5	3.4	1.34	4.7	0.91	1.1	0.53	3.0	0.41
277	2.73	11.16	45	332	43	3.1	4.4	10	10	3.6	1.39	5.1	0.90	1.2	0.46	2.8	0.49
278	2.61	9.25	38	267	37	<1	4.0	9.5	9.7	3.3	1.31	3.8	0.75	1.1	0.36	2.6	0.43
279	2.85	10.41	43	307	43	1.4	4.0	10	11	3.6	1.45	5.3	0.81	1.2	0.45	3.0	0.53
280	2.88	9.57	44	332	45	2.8	4.2	13	11	3.7	1.47	5.0	0.84	1.3	0.51	3.2	0.57
281	2.89	10.34	42	284	42	<1	4.2	10	10	3.5	1.39	5.1	0.87	1.0	0.52	3.0	0.41
282	2.77	10.53	41	281	41	<1	4.1	9.5	11	3.4	1.33	4.7	0.78	1.3	0.46	3.0	0.46
283	2.81	10.07	42	314	41	2.6	4.3	11	11	3.3	1.30	5.1	0.81	1.2	0.51	3.2	0.42
284	2.76	9.41	41	357	39	2.7	3.9	9.6	8.5	3.2	1.18	3.9	0.70	1.1	0.50	2.7	0.39
285	2.90	10.33	42	314	41	1.3	4.4	10	9.0	4.0	1.35	4.5	0.88	1.3	0.46	3.3	0.54
286	2.74	7.73	39	355	56	3.5	2.4	6.5	8.6	2.6	1.06	3.3	0.72	1.1	0.45	2.6	0.40
287	2.83	9.38	42	400	61	<1	2.6	8.1	9.4	2.8	1.21	3.7	0.78	1.1	0.43	2.5	0.45
288	2.81	13.02	45	126	46	3.4	4.2	12	10	3.8	1.47	6.2	1.1	1.2	0.51	3.4	0.57
289	2.77	11.10	44	129	43	2.6	4.3	13	11	3.7	1.44	4.6	0.88	1.4	0.58	3.2	0.55

TABLE 5a
Average Compositions of the Magmas Found at the EPR Sites, Leg 54

Hole	423		421		420		429A		427		422		428		428A	
Age (m.y.)	1.6		3.4		3.4		4.6		ca. 3.4		1.7		2.0		2.0	
Magma Group	423-1	423-2	421-1	421-2	420-1	429A-1	429A-2	427-1	422-1	422-2	422-3	428-1	428A-1	428A-2	429A-3	
Core Interval	5, CC to 7-1	8-1	2-1 to 3-1 (25 cm)	3-1 (110 cm) to 4-1 & bit	13, CC to 17-1	1-1 to 2-1 (14 cm)	2-1 (100 cm) to 3-1	9-1 to 10-3	7-1 to 9-1	9-2 to 9-5	10-1	5-4 to 6-2	1-1 to 1-2 (57 cm)	1-2 to 3-1 (36 cm)	3-1 to 7-2	
SiO ₂	50.79	50.38	49.97	51.09	50.64	49.93	50.55	50.05	50.26	49.26	50.27	49.90	50.03	50.57	50.60	
TiO ₂	2.14	2.09	2.63	2.13	1.93	1.17	1.62	2.58	1.58	1.41	2.03	1.56	1.59	1.56	1.52	
Al ₂ O ₃	13.65	13.60	13.51	13.17	14.18	16.00	14.35	13.79	14.09	15.38	13.65	14.70	14.85	15.16	14.52	
Fe ₂ O ₃	4.69	5.62	6.62	6.08	4.92	3.39	3.82	3.98	3.69	3.54	2.94	4.02	3.66	3.19	3.02	
FeO	6.60	6.53	6.60	5.43	6.25	5.20	7.63	8.88	6.59	5.44	8.00	6.38	6.70	6.91	7.14	
MnO	0.21	0.19	0.22	0.21	0.19	0.14	0.19	0.20	0.19	0.21	0.20	0.19	0.22	0.19	0.17	
MgO	6.68	6.28	5.98	6.61	6.64	7.29	7.18	6.60	7.89	8.35	7.25	7.48	7.57	7.22	7.89	
CaO	10.36	10.38	9.91	10.91	11.06	12.15	10.85	9.77	11.57	11.72	11.21	11.68	11.64	11.41	11.20	
Na ₂ O	2.70	2.77	2.61	2.62	2.53	2.46	2.50	2.97	2.71	2.76	2.72	2.60	2.65	2.59	2.50	
K ₂ O	0.36	0.37	0.55	0.50	0.43	0.11	0.29	0.09	0.12	0.20	0.31	0.14	0.10	0.25	0.16	
P ₂ O ₅	0.22	0.20	0.20	0.17	0.14	0.13	0.20	0.30	0.13	0.14	0.17	0.19	0.19	0.19	0.19	
H ₂ O [*]	1.05	0.85	1.24	1.20	1.12	1.22	0.56	1.03	0.83	0.92	0.96	0.60	0.69	0.78	0.82	
Total	99.72	99.26	100.04	100.12	100.03	99.19	99.74	100.24	99.65	99.33	99.69	99.44	99.89	100.02	99.73	
Trace elements in ppm																
Ni	60	49	56	72	82	139	58	53	56	112	65	67	65	67	67	
Cu	52	58	52	65	56	75	50	48	52	54	53	70	65	60	65	
Zn	97	98	100	98	100	67	82	86	74	66	65	77	75	68	68	
Y	38	45	51	48	44	21	31	45	31	24	31	27	28	26	26	
Sr	122	129	120	124	115	138	115	121	142	175	109	127	129	135	135	
Zr	158	162	205	178	161	65	103	191	114	104	144	103	103	100	98	
Rb	1	1	4	6	10	1	3	1	1	1	1	3	2	1	1	
Li	6	4	5	6	5	-	-	-	6	6	6	-	-	-	-	
FeO*/MgO ^a	1.66	1.85	2.13	1.65	1.61	1.13	1.54	1.89	1.26	1.03	1.51	1.34	1.32	1.35	1.25	
SI	32.10	29.89	27.56	32.03	32.74	40.25	34.13	29.94	38.24	41.94	34.64	36.99	37.20	36.38	38.66	

*Total iron as FeO.

TABLE 5b
Average Compositions of the Magmas Found at the Galapagos Rift Sites, Leg 54

Hole	424	424A	424B	424C	425						
Age (m.y.)	0.6 to 0.62				ca. 1.8						
Magma Group	424-1	424A-1	424B-1	424B-2	424C-1	425-1	425-2	425-3	425-4	425-5	425-6
Core Interval	4-6 to 7-1	4-1 (11-44 cm)	5-1 (58-91 cm)	5-2 (11 cm) 6-1 (115 cm)	2-1 (19 cm) 3-1 (56 cm)	7-1 (36-101 cm)	7-1 (133 cm) 7-2 (77 cm)	7-2 (102 cm) 8-1 (50 cm)	8-1 (97 cm) 9-1 (76 cm)	9-1 (100 cm) 9-2 (30 cm)	9-2 (118 cm) 9-3 (77 cm)
SiO ₂	50.87	51.85	50.72	51.25	50.92	51.04	51.09	50.16	50.43	50.57	50.18
TiO ₂	1.80	1.77	1.78	1.75	1.88	1.35	1.20	1.19	0.96	0.97	1.01
Al ₂ O ₃	12.91	12.83	13.02	13.47	12.83	13.78	14.00	14.14	14.32	14.53	14.14
Fe ₂ O ₃	3.12	2.32	3.44	2.77	2.13	3.01	3.14	3.66	3.06	3.93	3.65
FeO	9.98	10.70	9.67	10.30	10.83	9.05	8.30	7.55	7.18	7.23	7.30
MnO	0.21	0.22	0.20	0.21	0.23	0.19	0.18	0.17	0.16	0.17	0.17
MgO	6.44	5.98	6.09	6.57	6.63	7.60	8.08	8.08	8.41	8.19	8.39
CaO	10.36	10.52	10.04	9.98	10.70	11.43	11.74	11.96	12.11	11.77	11.95
Na ₂ O	2.40	2.34	2.44	2.33	2.29	2.17	2.00	1.87	1.74	1.87	2.18
K ₂ O	0.09	0.11	0.08	0.13	0.13	0.07	0.03	0.05	0.03	0.07	0.01
P ₂ O ₅	0.18	0.19	0.18	0.19	0.16	0.12	0.10	0.12	0.11	0.09	0.10
H ₂ O ⁺	1.00	1.49	1.91	0.92	0.70	0.75	0.74	0.65	0.85	0.75	0.73
Total	99.36	100.32	99.57	99.84	99.43	100.53	100.60	99.60	99.36	100.14	99.81
Trace elements in ppm											
Ni	48	52	58	52	33	52	55	66	67	61	82
Cu	59	63	62	60	51	62	65	71	71	75	72
Zn	101	111	111	96	116	95	78	73	74	85	74
Y	38	41	38	42	38	30	27	25	20	26	25
Sr	66	68	66	67	63	56	56	53	55	56	56
Zr	121	130	120	114	124	80	72	62	46	48	47
Rb	1	2	1	1	2	1	1	1	1	1	1
Li	6	6	—	—	—	—	—	—	—	—	—
FeO*/MgO ^a	1.99	2.14	2.10	1.95	1.92	1.55	1.38	1.34	1.18	1.31	1.26
SI	29.65	28.18	28.49	30.10	30.41	35.18	38.04	38.76	41.81	39.19	39.64

^aTotal iron as FeO.

basalts from these holes probably represent a quickly cooled portion of the same magma that gave rise to the doleritic unit.

The average compositions of magmas found in these holes are given in Table 5a, while Cores 428-1 and 2 are the averages of olivine basalts; Core 428A-3 is the average of doleritic rocks. The magma group of Cores 428-1 and 428A-1 are similar and differ from that of Core 428A-2 only with regard to K₂O content. The higher K₂O content of Core 428A-2 may not be a genetic feature but be related to later alteration, since in all other respects it is similar to the magma group of Cores 428-1 and 428A-1. As stated above, the olivine basalt sub-groups have slightly higher FeO*/MgO and lower SI value as compared with the sub-group of Core 428A-3, representing doleritic rocks.

Besides the major and trace element data, REE and some additional trace elements for these basalts are also given in Table 4; the rare-earth pattern for these basalts is shown in Figure 2. No significant differences occur in the total REE or their distribution with respect to depth of sample or type of basalt. All samples are depleted in lighter rare earths as compared with heavier ones. The La/Sm (e.f.) is always less than one, similar to ocean-ridge tholeiites described by Kay et al. (1970), Schilling (1971), and others.

Like REE, Sc, Cr, Co, Hf, Ni, Cu, Zn, Y, Sr, Zr, and Rb do not show any significant variation. In general, basalts from these holes are very similar to the upper doleritic unit from Hole 422. For a quick comparison, some of the data are tabulated below:

	Hole 422, Magma Group, Core 422-1	Holes 428 and 428A, Average of 17 Analyses
SiO ₂	50.26	50.36
TiO ₂	1.58	1.55
Al ₂ O ₃	14.09	14.81
MgO	7.89	7.53
CaO	11.57	11.46
Na ₂ O	2.71	2.58
Zr	114	101
Sr	142	132
Y	31	26
FeO*/MgO	1.26	1.30
SI	38.24	37.30

Hole 429A

Basalts from this hole belong to two chemically distinct types. The average chemical composition of these types is given in Table 5a. The younger olivine basalts from the upper part of the hole (Magma Group, Core 429A-1) are low-Ti, low-K basalts. The Al and Ca contents of these basalts are also high (Al₂O₃ = 16%, CaO = 12.15%). The FeO*/MgO ratio is 1.13, and the SI value is 40.23. Compared with these, aphyric basalts from the lower part of the hole (magma group, Core 429A-2) have low to moderate Ti (1.62%), relatively high K, and lower Al and Ca. The FeO*/MgO ratio of these basalts is 1.54, and SI value is 34.13.

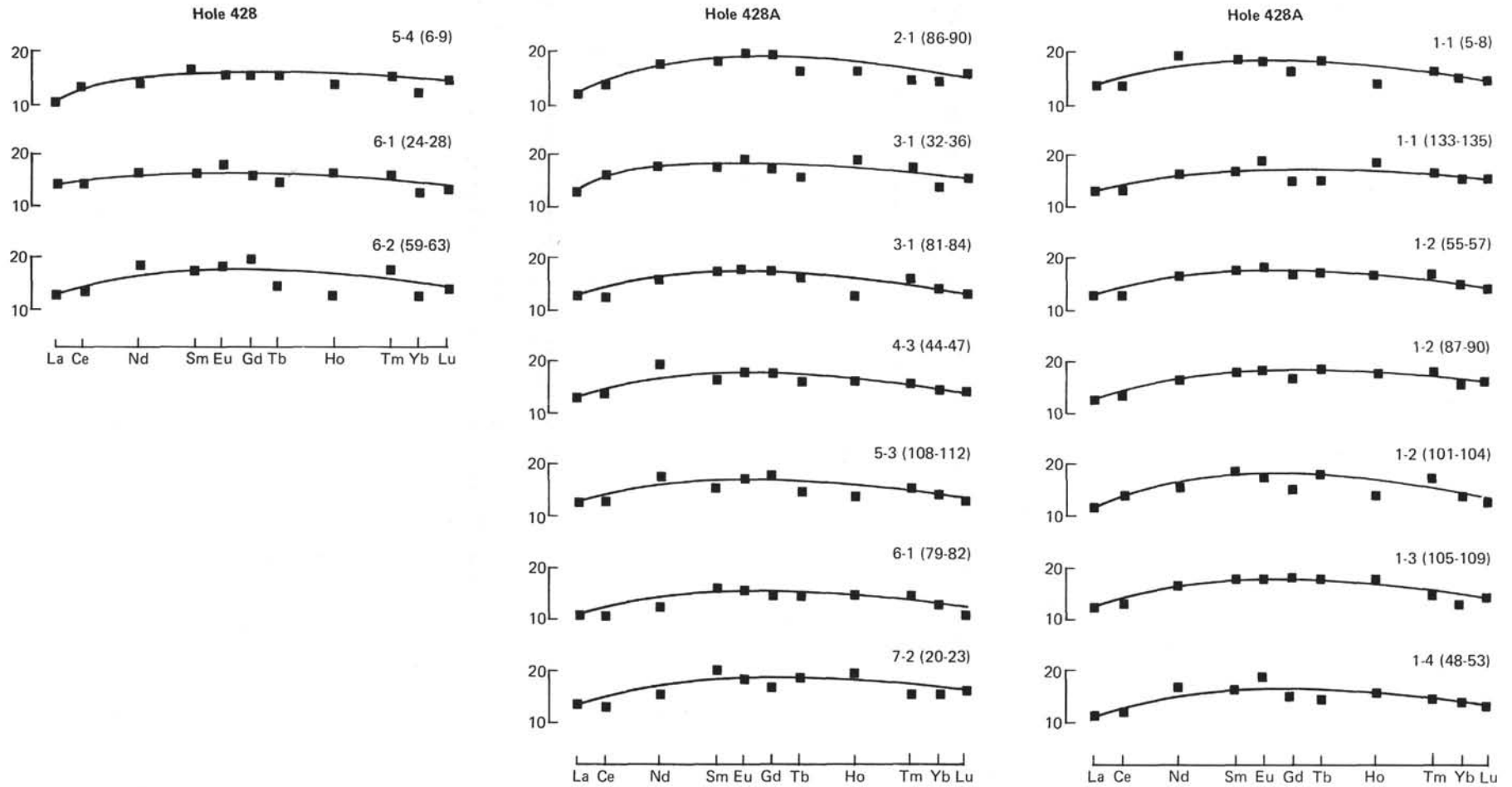


Figure 2. REE chondrite-normalized distribution patterns of basalts from Holes 428 and 428A (Sample intervals in cm.)

There are also significant differences in the trace element contents of these groups. In group 1, Ni, Cr, and Cu are significantly higher and Zr, Y, and Rb lower than in group 2.

The REE patterns of these basalts are given in Figure 3. The total REE for group 1 is half the value for group 2; however, all patterns are depleted in light REE. The La/Sm (e.f.) for group 1 is 0.58, and for group 2, 0.71. The La/Yb (e.f.) is 0.58 and 0.76, respectively.

Petrographically and chemically, group 2 basalts from this hole appear to be closely related to other normal fabric basalts from Holes 420, 421, and 423; however, they are more primitive than the basalts from Holes 420, 421, and 423. On the other hand, group-1 magma from Hole 429A differs significantly from EPR normal fabric basalts — with respect to both their major oxide and trace element chemistry, and it may not therefore have been formed at the EPR crest. The magnetic data of these basalts also suggest that they are younger than indicated by the marine magnetic anomaly for Hole 429A. To a certain extent, these basalts resemble the group-2 basalts from Hole 422. In the latter hole, also the doleritic unit postdates the rocks that produced Anomaly 2 (Olduvai normal event, 1.79 to 1.64 m.y.), although the hole is located well within the Anomaly 2 (See Site Report for Holes 422 and 429A).

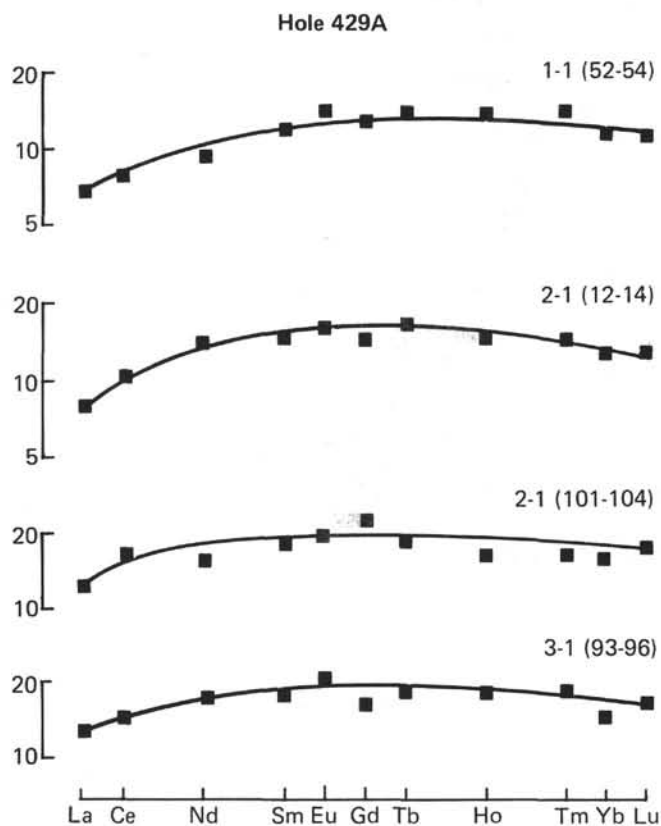


Figure 3. REE chondrite-normalized distribution patterns of basalts from Hole 429A (Sample intervals in cm).

Hole 427(SFZ)

Four analyzed samples of basalts from this hole are identical in their chemistry, which is in keeping with their uniform petrography. They can be characterized as high-Ti, high-Fe basalt. The FeO*/MgO ratio of these basalts varies from 1.80 to 1.97, and the SI value from 30.17 to 28.71.

The REE patterns of these basalts are given in Figure 4. All the basalts from this hole are LREE-depleted; however, depletion of LREE is less than at Site 428 and 429 basalts. The total REE is also almost double that of the Site 428 and 429 basalts.

Amongst trace elements, Zr shows the highest concentration (186–194 ppm). Y is also high (42–46 ppm). Cr, Ni, and Cu concentrations are low.

From *Glomar Challenger* underway records, we know that some of the troughs in the SFZ are characterized by a relatively flat floor and reflective basement. These structures may represent intact down-faulted blocks into which flows had been ponded. Hole 427 was drilled to determine if the chemistry and petrography of trough rocks were similar or comparable to those of fabric basalts erupted from the EPR proper, namely basalts from Holes 420, 421, 423, and 429A.

Hole 427 is located on the southern flank of the SFZ (Figure 1) and may originally have belonged to the block of oceanic crust to the south. Assuming a spreading rate similar to that of the EPR north of the fracture zone, the calculated age of the site comes to approximately 3.4 m.y. (distance of Hole 427 from the ridge crest is 196 km). It should be mentioned here that the age of sediments at this site ranges from only 0.2 to 1.2 m.y. (see Site Report).

If the basalts have an age in the order of 3.4 m.y., and if the nature of basalts erupted at the EPR proper,

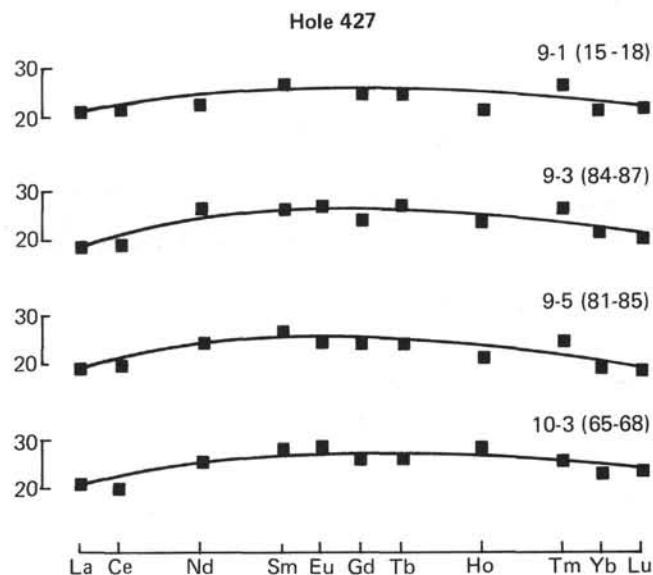


Figure 4. REE chondrite-normalized distribution patterns from Hole 427 (Sample intervals in cm).

north and south of the fracture zone, are similar, then the chemistry of Hole 427 basalts might well be similar to that of Hole 420 and 421 basalts.

Table 6 presents a comparison of analytical data from Hole 427 with Holes 420 and 421 and the EPR crest north and south of the SFZ. This shows that: 1) Broadly speaking all analyses are of high-Ti, high-Fe, low-Al, and low-Ca basalts. 2) Except for K, Hole 427 basalts are similar to glassy basalts from Hole 421; the total alkalis in both, however, are of similar order. 3) There are significant differences between the two dredged EPR crest basalts (SD5-1 and V2023) and present SFZ basalts in respect to enrichment level of Ti and K.

Galapagos Rift

Holes 424, 424A, 424B, and C

These four holes form a north-south transect across a geothermal mounds field approximately 22 km south of the GR. The magnetic crustal age varies from 0.6 m.y. at Hole 424C to 0.62 m.y. at Hole 424A. Holes 424 and 424A are located on mound-like features, and the other two holes are located off mounds. Analyses of 24 samples from these sites are given in Tables 2 and 3, and the averages are given in Table 5b. An analysis of data in these tables reveals that there are no significant differences in the composition of basalts from these holes; only Hole 424B basalts show minor differences in chemistry downhole (they form two groups). The uniform chemistry of these basalts is in keeping with their uniform petrography.

All basalts from these holes have high Fe, high Ti, and low Al. Another interesting feature of their chemistry is their extremely low K, despite very high Fe, Ti, and a high FeO*/MgO ratio. The total alkali content of

these basalts is generally below 2.60 per cent. These chemical features are also common to some of the dredged basalts reported from this area by Anderson et al. (1975) and Schilling et al. (1976). Two of the dredge hauls — Southtow 7, D-17, and Cocotow 4, 6D-1 and 6D-2 — together with Holes 424, 424A, B, and C, form a north-south transect across the GR at 86° W latitude. Fe and Ti contents of Cocotow 4, 6D-1 and 6D-2 are similar to Site 424 basalts, but the Southtow 7, D-17 basalts have higher Ti and slightly lower Fe than Site 424 basalts. The low Al in high-Fe basalts is a feature common to both drilled and dredged samples.

Like major oxides, trace elements in these basalts show only limited variation. Their Zr content varies from 114 to 130 ppm. Strontium in these rocks is extremely low (63 to 68 ppm); Y is about 40 ppm. Concentrations of Ni and Cu are also low.

In comparison with EPR normal fabric basalts from 9° N, these basalts are more fractionated as is evident from their higher total iron, and higher FeO*/MgO ratio; despite this, their total alkalis, Zr, Rb, and Sr contents are much lower than those of the EPR normal fabric basalts.

Hole 425

Basalts from this hole (located 84 km north of Site 424 on the northern flank of the GR), show somewhat diverse chemistry. The hole lies just beyond the Olduvai magnetic boundary (slightly older than 1.8 m.y.) in a sediment-filled topographic depression characterized by high heat flow (~5 HFU; Williams et al., 1974); furthermore, it is within, or very close to, the zone of large-amplitude magnetic anomalies associated with the GR. Although the hole lies on Matuyama-age reversed, magnetized crust (very close to the boundary of the normal Olduvai event), rocks in the upper part of the hole show normal polarity and in the lower part reverse polarity. It is not unlikely that the upper part belongs to the Olduvai normal event and the lower part belongs to Matuyama. In addition, the deviations from zero inclinations are considerable in this hole. Peterson and Roggenthen (this volume) believe these magnetic features to be a consequence of tilting.

Chemical analyses of 14 samples of basalts from this hole are given in Tables 2, 3, and 4. On the basis of petrographic types, the rocks can be grouped into six chemical sub-groups. The average composition of these sub-groups is given in Table 5b. The data reveal that the basalts from this hole generally have low Ti, moderate Fe, and relatively high Mg. The Al₂O₃ content in these basalts is about 14 per cent, and the CaO content about 12 per cent. The total alkalis content is the lowest for all sites drilled during the Leg. In comparison with the basalts from Site 424, these rocks are much poorer in Ti and Fe and richer in Mg. Their alkali content also is much lower than that of the Site 424 basalts.

Chemical types of Cores 425-1, 2, 3, and 4 (Table 5b) belong to petrographic types 1, 2, 3, and 4 (Appendix),

TABLE 6

Comparison of Analytical Data from Hole 427 with Holes 420, 421, and EPR Crest North and South of Fracture Zone

	1	2	3	SD5=1	V2023
SiO ₂	50.71	49.97	50.05	50.70	48.30
TiO ₂	2.13	2.63	2.58	2.19	2.26
Al ₂ O ₃	13.65	13.51	13.79	13.60	14.30
FeO (total Fe)	11.08	12.56	12.46	12.71	11.70
MnO	0.20	0.22	0.20	0.22	—
MgO	6.52	5.98	6.60	6.94	6.70
CaO	10.80	9.91	9.77	11.48	10.10
Na ₂ O	2.60	2.61	2.97	3.57	2.75
K ₂ O	0.48	0.55	0.09	0.27	0.18
P ₂ O ₅	0.16	0.20	0.30	0.25	—
Ni	73	56	53	51	58
Sr	120	120	121	185	107
Zr	175	205	191	—	—

Notes:

1 = Average of Holes 420 and 421.

2 = Average of glassy basalts from Hole 421.

3 = Average of Hole 427 basalts.

SD 5-1 = EPR crest north of SFZ (Batiza et al., 1977).

V 2023 = EPR crest south of SFZ (Kay et al., 1970).

respectively; the chemical type of Core 425-5 is again aphyric basalt (petrographic type 1), and the chemical type of Core 425-6 represents the petrographic type 5. The rocks belonging to the chemical type of Cores 425-1, 2, and 3 have normal polarity, and those belonging to Cores 425-4, 5, and 6 have reversed polarity. Aphyric basalts constituting type 1 differ from types 2 and 3 (pyroxene-plagioclase sparsely phyrlic basalts and phyrlic-glomeroporphyritic basalts) in having higher titanium, higher total iron, alkalis, and lower magnesium. Slight differences or none at all between types 2 and 3 are in keeping with their similar mineralogy. The chemical type of Core 425-4 differs significantly from the overlying types in having lower Fe, lower Ti, and higher Mg. The FeO^*/MgO ratio of this group is also much lower than that of the others. These changes in chemistry can be traced to the presence of olivine in the glomerocrysts of these basalts. Aphyric basalts below this unit (chemical group of Core 425-5) differ from aphyric basalts from type 1 in having higher MgO and lower TiO_2 and total iron. This chemical type is similar to that of Core 425-6 found at the bottom of the hole and probably represents chilled margin of the petrographic type 5. The REE data of the last two sub-groups given in Table 4 support this contention. An interesting feature of the REE data is the extreme depletion of LREE as compared with HREE. The normalized patterns of these basalts given in Figure 5 are strongly LREE-depleted; however, HREE show an enrichment of about 20 times of chondritic values.

Cores 425-1, 2, and 3 show systematic variation in downhole chemistry at this hole. TiO_2 decreases from 1.35 to 1.19 per cent, total iron (as FeO) from 11.76 to 10.84 per cent, and alkalis from 2.24 to 1.92 per cent. Al_2O_3 , MgO, and CaO show an increase from 13.78 to 14.14 per cent, 7.60 to 8.08 per cent, and 11.43 to 11.96 per cent, respectively. FeO^*/MgO decreases from 1.55 to 1.34, and SI increases from 36.18 to 38.76. Amongst the trace elements, Ni shows an increase from 52 to 66 ppm, and Zr decreases from 80 to 62 ppm. The chemistry of Core 425-4 immediately below Core 3 may represent a chemical break, because its MgO is significantly higher and total iron and TiO_2 are lower than in unit 3. The FeO^*/MgO ratio of this unit is 1.18 and the SI value is 41.81. Below this unit, however, the ratio FeO^*/MgO again shows an increase, and the SI value a decrease. If the chemical unit of Core 425-4 is altogether neglected, then downhole variation in chemistry becomes more systematic; that is, from the top to the bottom TiO_2 decreases from 1.35 to 1.01 per cent, total iron (as FeO) from 11.76 to 10.58 per cent, and MgO increases from 7.60 to 8.39 per cent. The ratio FeO^*/MgO decreases from 1.55 to 1.26, and the SI value increases from 35.18 to 39.64. Amongst trace elements, Ni increases from 52 to 82 ppm and Zr decreases from 80 to 47 ppm.

In view of these facts, it is not unlikely that the entire sequence of rocks found at this site was erupted at the transition of the Matuyama and the Olduvai normal event, and that the older Matuyama rocks have a nega-

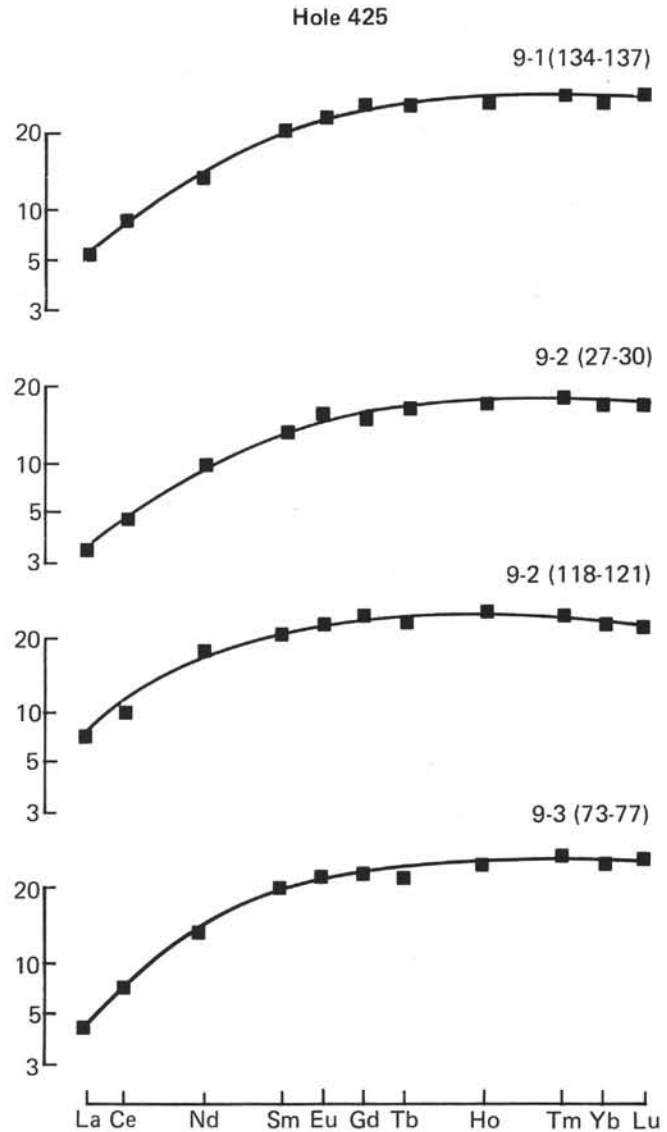


Figure 5. REE chondrite-normalized distribution patterns of basalts from Hole 425 (Sample intervals in cm).

tive polarity and the younger ones belonging to Olduvai have normal polarity. In general, it can be said that the rocks with negative polarity are less evolved than those having positive polarity.

Chemical Variation Across the Galapagos Rift

Hole 425 on the northern flank of the Rift and Site 424 on the southern flank, along with the previously reported dredge haul Southtow 7, D-17 and Cocotow 4, 6D, form a north-south transect at 86° W. De Steiguer 41, D1A, D1B, D3A, D3B, and D4 form another transect at $85^\circ 30'$ W. Data from these sites offer, therefore, an opportunity to study chemical variations across the GR. Furthermore, both the drilled sites and all the dredges are located within, or very close to, the zone of high-amplitude magnetic anomaly associated with the GR between 85° and 88° W. According to Anderson et

al. (1975), this zone is the result of intrusion and extrusion of large amounts of Fe-rich tholeiite at the ridge crest from the time of the formation of Anomaly 2 up to the present.

Figure 6 shows variation in certain elements and ratios with distance from the ridge crest around 86° W. Generally speaking, samples close to the ridge crest are rich in Fe and Ti; away from the crest their concentra-

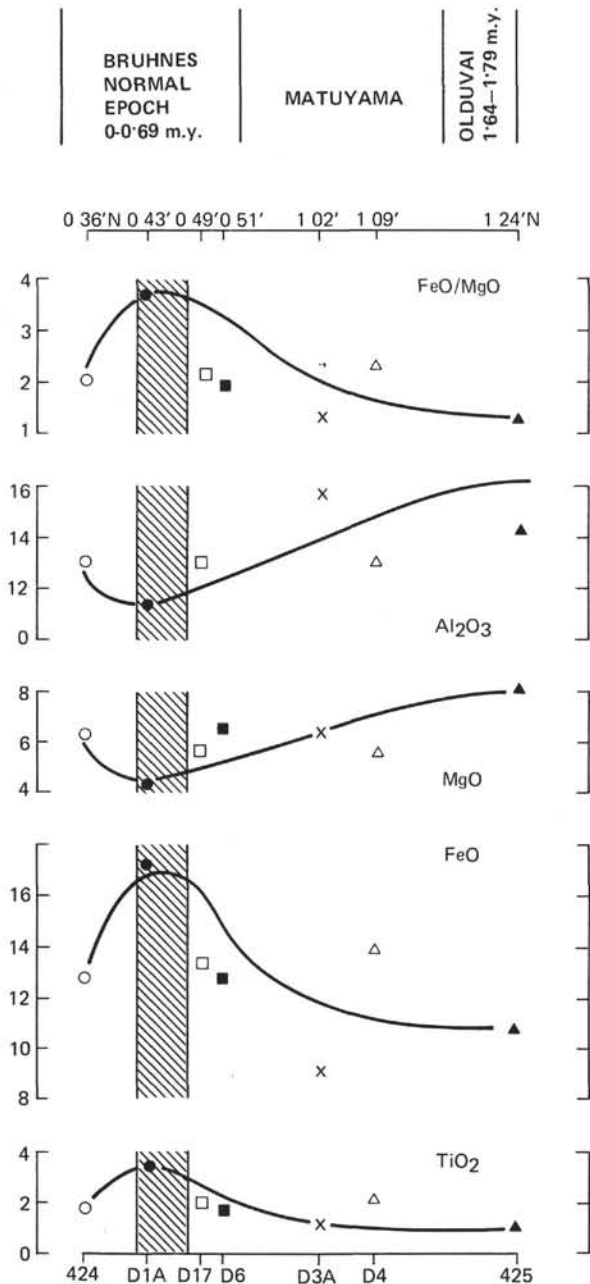


Figure 6. Variations in the concentrations of selected major oxides and in FeO/MgO ratio across the GR at 86°W latitude. The shaded area indicates the ridge crest region. Site 424 and 425 data are from the present work, D-17 data are from Anderson et al. (1975), and D1A, D6, D3A, D4 data are from Schilling et al. (1976).

tion decreases. Likewise, the ratio FeO*/MgO shows a progressive decrease away from the crest. On the other hand, Mg and, to certain extent, Al show a progressive increase away from the crest. This is contrary to the view of Schilling et al. (1976) who report "There seems to be no systematic variation in Fe and Ti enrichment with distance or age across the ridge in the 85°–87° W area."

NOMENCLATURE AND CLASSIFICATION OF BASALTS

Generally, petrographic (phenocryst contents) and chemical criteria are used for classifying basaltic rocks from an oceanic environment. In this paper, we do not use petrographic criteria because the large number of rocks studied by us usually lack phenocrysts and are either glassy or very fine grained. The chemical schemes for classifying or distinguishing basaltic rocks are either based on empirical boundaries such as the tholeiite/alkali basalt boundary proposed by Chayes (1966) and the alkali-silica diagram (Kuno, 1968; MacDonald and Katsura, 1964), or are based on the normative composition of basalt or its parental liquid. Normative composition, particularly the degree of silica saturation, as indicated by the presence or absence of quartz, nepheline, or olivine in the norm, can in principle apply to any basaltic liquid, provided the oxidation state of iron is taken into account. Furthermore, normative classifications are useful in relating natural (especially nearly glassy) basalts to the results of experimental petrology.

Following the procedure of Coombs (1963), basalts in this study are classified according to their norm. For the purpose of the norm calculation, instead of choosing an arbitrary value of 1.5 per cent Fe₂O₃, as was done by Kay et al. (1970) and some others, we have decided to fix the ratio Fe₂O₃/FeO at 0.15, since the lowest observed Fe₂O₃ content of unaltered submarine basalt ranges from 1.0 to 1.5 per cent and the total Fe content is in the vicinity of 10 per cent. We chose a low Fe₂O₃/FeO ratio for two reasons: (1) we find large variation in Fe₂O₃/FeO with almost constant total Fe, and (2) the H₂O content of these basalts is more than 0.5 per cent, a value normally reported for the ocean-ridge basalts. Furthermore, since it is unlikely that shallow magmatic processes result in the reduction of an oxidized liquid, we have assumed that the Fe₂O₃ contents of ocean-ridge basalt parental liquids are similar to the observed low values.

The present basalts outlined in Figure 7 are highly variable in normative chemistry. There are no rocks with alkalic affinities, but most of them are quartz-normative. This finding is contrary to that of Chayes (1965) and Kay et al. (1970), who report that most of the ocean-ridge tholeiites are neither quartz- nor nepheline-normative. To a certain extent our finding is similar to that of Kempe (1975), who reports that more than 25 per cent of the drilled oceanic basalts are quartz-normative; in our study, however, over 70 per cent of samples are.

Except for a few samples, all EPR normal fabric basalts are quartz-normative with a diopside (di) max-

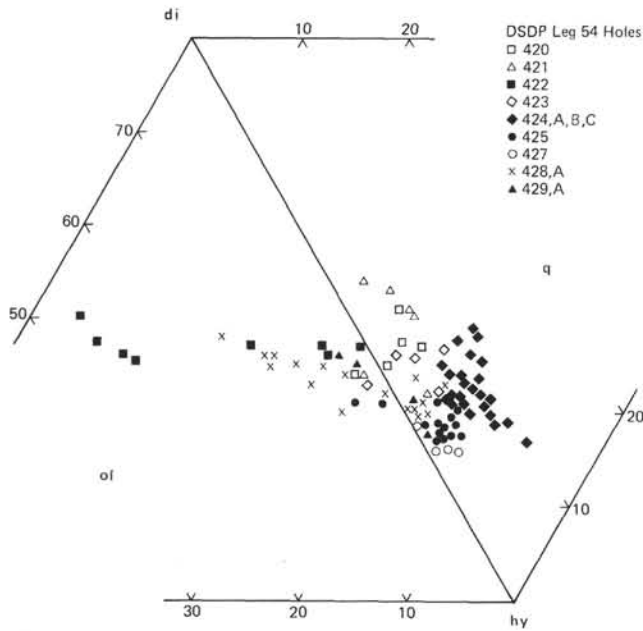


Figure 7. *ol-di-hy-q* diagram for Leg 54 basalts.

imum of about 53 per cent. SFZ basalts (Hole 427) are also quartz-normative, but their di maximum is about 44 per cent. On the other hand, basalts from OCP moat sites (Holes 422, 428 and 428A) by and large are olivine-normative with a di maximum of about 57 per cent, a figure which is typical of most drilled basalts (see Kempe, 1975). The GR sites are also quartz-normative; however, their di maximum is much lower — about 44 per cent.

On the alkali-silica diagram (Figure 8), all samples fall in the field of tholeiites as given by Macdonald and

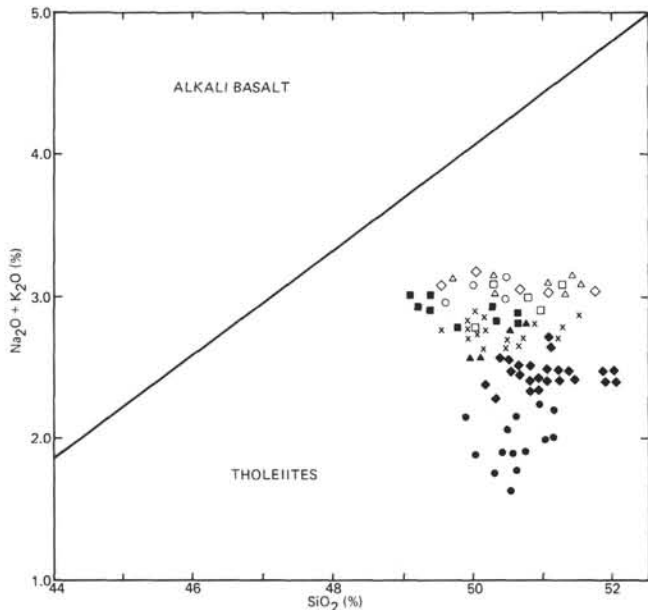


Figure 8. *Alkali-silica* variation diagram for Leg 54 basalts. The tholeiites/alkali basalt boundary is after Macdonald and Katsura (1964). Hole symbols are same as in Figure 7.

Katsura (1964). It is interesting that the samples from the GR plot in a field less alkalic than that of EPR samples. The variation in total alkalis is large, in spite of limited variation in silica.

In recent years a number of schemes using trace elements have been propounded to relate basic volcanic rocks to magma type and tectonic setting. Cann (1970) and, later, Pearce and Cann (1971 and 1973) have propounded schemes based on Ti, Zr, Y, and, for less altered rocks, Sr. A scheme using TiO_2 , K_2O , and P_2O_5 was put forward by Pearce (1975), and one using Ti, Zr, Y, Nb, and P by Floyd and Winchester (1975). Smith and Smith (1976) have discussed the usefulness of these various schemes in the classification of basalts.

There is a positive correlation between the pairs Ti-Zr and Ti-Y in ocean-floor basaltic rocks; tholeiites may show a proportional trend, whereas alkali basalts have a horizontal trend. Figures 9 and 10 are TiO_2 -Zr and TiO_2 -Y plots of present basalts along with some of the data for DSDP Legs 16, 34, 37, and 52. The diagrams show a remarkable positive correlation between these element pairs, a finding which is similar to that of Cann (1970) who reports positive correlation between those element pairs in ocean-floor basaltic rocks from different ocean areas. Furthermore, amongst the Leg 54

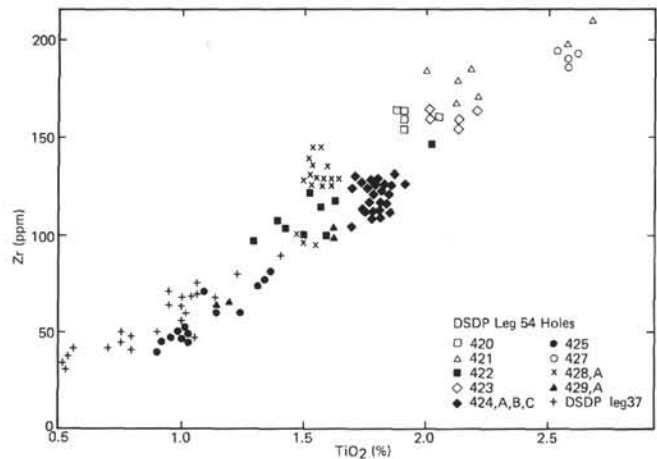


Figure 9. *Covariation of TiO_2 and Zr* for Leg 54 basalts. DSDP Leg 37 data are our unpublished data.

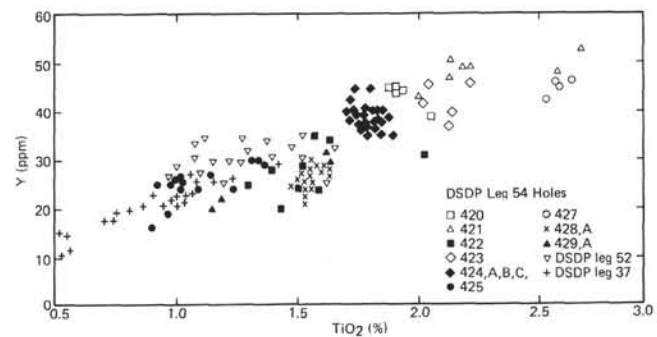


Figure 10. *Covariation of TiO_2 and Y* for Leg 54 basalts. DSDP Leg 37 and 52 data are our unpublished data.

basalts, EPR normal fabric basalts and SFZ basalts have the highest concentrations of Ti, Zr, and Y.

The pair TiO_2 - P_2O_5 also shows two trends: one for the tholeiitic suite, where an increase in TiO_2 is matched by a proportional increase in P_2O_5 , and the other for the alkalic suite where there is a threefold increase in P_2O_5 with each doubling of TiO_2 . Both trends converge near 1 per cent TiO_2 and 0.1 per cent P_2O_5 , and it is therefore not possible to distinguish rocks from the two suites with extremely low Ti and P by means of this plot. Figure 11 is a TiO_2 - P_2O_5 diagram of the present rocks. Like the Ti-Zr and Ti-Y diagrams, this one also shows a proportional trend. The dashed line is the ridge crest trend.

The K_2O - TiO_2 diagram (Figure 12) has been used to distinguish, and speculate on, the relationships between different types of basaltic rocks. It is interesting that the data from GR sites fall on a narrow K_2O and wide TiO_2 range, whereas those from EPR sites show a near-proportional trend; the variation seems to be a continuous one. Furthermore, the SFZ basalts plot in a field of their own.

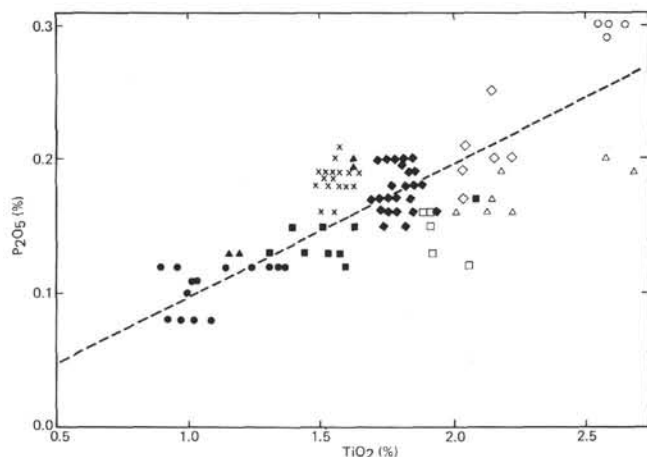


Figure 11. Covariation of TiO_2 and P_2O_5 for Leg 54 basalts. Dashed line indicates the ridge crest tholeiites trend. Hole symbols are same as Figure 7.

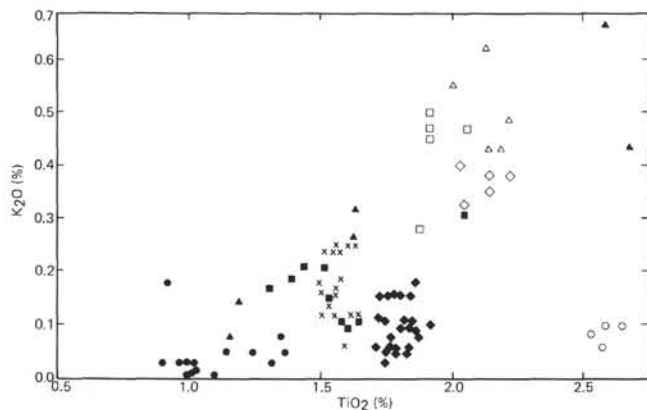


Figure 12. K_2O - TiO_2 variation diagram for Leg 54 basalts. Hole symbols are same as in Figure 7.

Concentrations of individual elements have also been used to characterize rocks from mid-oceanic ridges. Low K_2O and SiO_2 and high Al_2O_3 contents have all been put forward as characteristics of these rocks (Engel et al., 1965; Nicholls, 1965; Green and Ringwood, 1967; Kay et al., 1970; and Cann, 1971). None of the samples studied can be called high-alumina basalt, since the Al_2O_3 content of the present samples is commonly about 14 per cent. The range of K_2O is also fairly large, 0.01 to 0.6 per cent. The Si is generally above 50 per cent. Thus, the characterization by Engel et al. (1965) of ocean ridge basalts as being high in Al, low in K and Si, is not supported by the present data. Table 7 compares the averages of the present work with the averages given by Engel et al. (1965) as well as other averages from the Atlantic, Pacific, and Indian oceans. The table clearly reveals that present basalts are lower in Al and much higher in Ti and Fe as compared with the average oceanic tholeiite of Engel et al. (1965). In comparison with the Atlantic, the present basalts have higher Fe and Ti and lower Al and Mg. The present EPR normal fabric basalt average matches closely the EPR average of Melson et al. (1976), except for the Ti and K contents which are higher. On the other hand, when all EPR sites of Leg 54 — that is, normal fabric basalt, OCP moat basalt, and SFZ basalts — are taken together, the average comes very close to that of Melson et al. (1976), except for Fe which is lower. As regards the GR basalts, they appear to be a type in themselves characterized by extremely low Al, low Mg, and low total alkalis as well as high Fe. In the light of this, we suggest that use of "oceanic tholeiite" as a blanket term for ocean-floor basalts be dropped and that the latter be referred to as olivine tholeiite, quartz tholeiite, or high-alumina tholeiite, as the case may be. The present basalts are olivine and quartz tholeiites.

DISCUSSION AND CONCLUSIONS

We have shown that Leg 54 basalts have highly variable petrography and chemistry. All EPR normal fabric basalts are cryptocrystalline to fine-grained aphyric plagioclase-pyroxene basalt. The OCP moat basalts by and large are fine- to medium-grained plagioclase-pyroxene \pm olivine basalts. The SFZ basalts are fine- to medium-grained plagioclase-pyroxene basalts. The normal fabric basalts show textures ranging from hyalopilitic to intersertal. The OCP moat basalts and SFZ basalts have intersertal to ophitic texture. The GR basalts from Site 424 are similar to EPR normal fabric basalts in their petrography. The largest petrographic variation at any site of Leg 54 is among Hole 425 basalts. On the basis of texture and mineralogy, basalts from this hole can be grouped into four distinct petrographic types.

There are also significant differences in chemistry and normative mineralogy of basalts from various regions. EPR normal fabric basalts and SFZ basalts are high-Ti, moderate to high-Fe quartz tholeiites with low Ni and high Zr. The OCP moat basalts, on the other hand, are low- to moderate-Ti, low- FeO^*/MgO olivine tholeiite. Their Y and Zr are significantly lower than the

TABLE 7
Average Compositions of Oceanic Basalts and Basaltic Glasses Related to Spreading Ridges in the Atlantic, Pacific, and Indian Oceans

	1	2	3	4	5	6	7	8	9	10	11
SiO ₂	50.67	50.55	50.33	50.65	50.20	50.05	50.84	50.19	49.94	49.61	50.73
TiO ₂	1.28	1.69	1.81	2.07	1.52	2.58	1.54	1.77	1.51	1.43	1.19
Al ₂ O ₃	15.45	13.95	14.34	13.71	14.78	13.79	13.44	14.86	17.25	16.01	15.15
FeO*	9.67	11.04	10.36	10.89	9.70	12.46	11.94	11.33	8.71	11.49	10.32
MgO	8.05	7.12	7.17	6.57	7.72	6.60	7.05	7.10	7.28	7.84	7.69
CaO	11.72	11.00	11.09	10.69	11.52	9.77	10.88	11.44	11.68	11.32	11.84
Na ₂ O	2.51	2.46	2.64	2.61	2.62	2.97	2.22	2.66	2.76	2.76	2.32
K ₂ O	0.15	0.18	0.26	0.43	0.17	0.09	0.08	0.16	0.16	0.22	0.14

Notes:

- 1 = Atlantic 155 glass analyses, including FAMOUS data and DSDP Leg 37 (Bryan et. al., 1976).
- 2 = Equatorial East Pacific, Leg 54, 89 basalt analyses (this work).
- 3 = EPR, Leg 54, all sites around 9°N, 51 basalt analyses (this work).
- 4 = EPR normal fabric basalt, Leg 54, 20 basalt analyses (this work).
- 5 = OCP moat basalt, Leg 54, 25 basalt analyses (this work).
- 6 = SFZ basalt, Leg 54, four basalt analyses (this work).
- 7 = GR, Leg 54, 38 basalt analyses (this work).
- 8 = EPR, 38 glass analyses (Melson et al., 1975).
- 9 = Average oceanic tholeiite (Engel et al., 1965).
- 10 = Average oceanic tholeiite (Cann, 1971).
- 11 = Indian Ocean, 10 glass analyses (Melson et al., 1975).

EPR normal fabric and SFZ basalts. The GR basalts, insofar as their major oxides are concerned, display the complete chemical spectrum of the EPR normal fabric basalts, OCP moat basalts, and the SFZ basalts, except that their total alkalis are lower. Site 424 basalts are high-Ti, high-Fe quartz tholeiite, and Hole 425 basalts are low-Ti, low- to moderate-Fe quartz tholeiite. The presence of normative quartz in Hole 425 basalts is a consequence of their low alkalis. Another characteristic feature of GR basalts is their extremely low Sr and low to moderate Zr, despite high Ti and Fe.

The old concept that the deep ocean floor consists of basaltic rocks that are more or less uniform in composition and represent a primary magma composition is no longer valid. During the past few years several workers have demonstrated that ocean-floor basaltic rocks have systematic chemical differences and often show a moderate iron enrichment trend of fractionation oblique to the FeO-MgO side of an AFM diagram. The minerals participating in the shallow fractionation process have generally been inferred to be olivine and plagioclase (Kay et al., 1970; Miyashiro et al., 1969; Shido et al., 1971; Scheidegger, 1973; Schilling, 1975). Bunch and La Borde (1976), Clague and Bunch (1976) and Batiza et al. (1977) have noted the importance of clinopyroxene as fractionating phase and have propounded models with clinopyroxene and plagioclase as the dominating phases, with subordinate olivine for basalts occurring at east Pacific mid-ocean spreading centers. Furthermore, these authors have demonstrated that high-Fe and Ti basalts as well as ferrobasalts occurring at these centers can be derived by fractionation from normal mid-ocean ridge tholeiites.

According to Kempe (1975), in many of the DSDP basalts "differentiation patterns in moderately long drilled basalt cores show two main types of fractionation with respect to Fe/Mg and (normative) Ab/An.

Enrichment in iron and albite normally occurs upward (? within each flow), while sudden reversal of this trend may indicate new effusions of magma from its source. Repetitive step-like patterns thus result". Miyashiro (1975) reports that the FeO*/MgO ratio for abyssal tholeiites varies from 0.8 to 2.1, but most of the fresh samples have a ratio less than 1.7. Analytical data in Table 3 reveal that the FeO*/MgO ratio of the present rocks is highly variable, ranging from 1.0 to 2.14. The EPR normal fabric basalts show a variation from 1.50 to 1.80, except for two samples from Hole 421 which have a ratio above 2.0. The OCP moat basalts have lower FeO*/MgO than normal fabric basalts, the range being 1.0 to 1.40. Basalts from the SFZ (Site 427) also show high FeO*/MgO. GR basalts show considerable variation, while at Hole 425 the ratio varies from 1.13 to 1.54; at Site 424 the ratio varies from 1.89 to 2.14. As to the downhole variation at different sites, the reversal of trends as pointed out by Kempe (1975) also occurs in some of our drill holes.

To further test the possibility of crystal fractionation, the data have been plotted on an AFM diagram (Figure 13). This reveals that (1) there are two trends, one marked by the EPR sites and the other by the GRZ sites, (2) the Galapagos samples plot in a field which is less alkalic than that of EPR basalts, (3) both trends are slightly oblique to the MgO-FeO side of the AFM triangle and indicate a moderate iron enrichment, (4) EPR normal fabric basalts and SFZ basalts are more enriched in iron and alkalis than OCP moat basalts, (5) there seems to be a gap between the normal fabric and moat fields if the two samples from the lower part of Hole 429A and the sample from the bottom of Hole 422 are neglected, (6) the largest variation for any site is shown by the samples from Hole 425, and (7) Site 424 samples are more enriched in iron than Hole 425 samples and there is a gap between the two. The difference in Fe enrich-

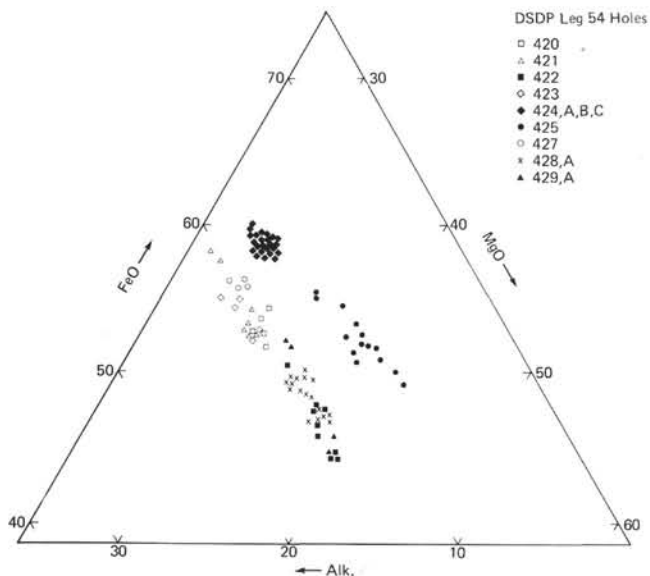


Figure 13. AFM diagram of Leg 54 basalts.

ment at two GR sites may be related to the respective ages of the basalts at these sites; the younger Site 424 basalts are more enriched in Fe than the older Hole 425 basalts.

In Figure 14 we compare the present data with North Atlantic data. It is interesting that (1) EPR normal fabric basalts mark a continuation of the North Atlantic trend and plot in a more iron-enriched field than the latter, (2) OCP moat basalts plot in the field of North Atlantic basalts, (3) the Galapagos samples, despite higher Fe enrichment, are clearly less alkalic than the North Atlantic basalts.

Generally speaking, basalts from modern ridges differ from one another, especially in terms of FeO*/MgO

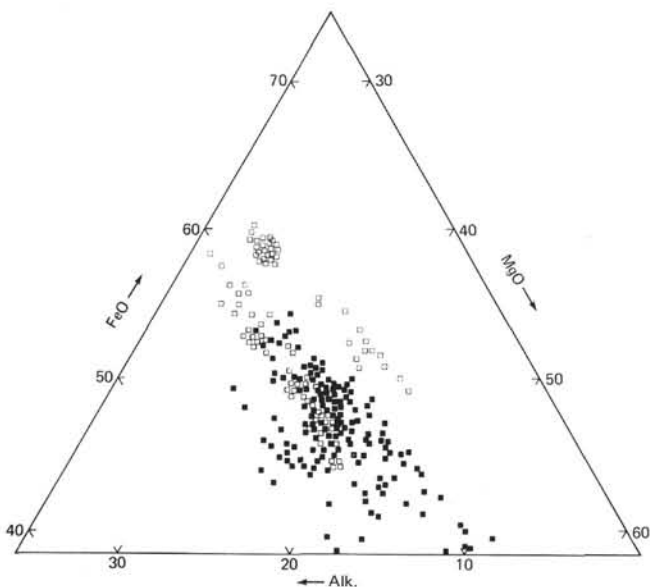


Figure 14. AFM diagram comparing Leg 54 basalts with North Atlantic basalts. Open squares are Leg 54, and solid squares are North Atlantic data.

and TiO₂. In Figure 15 we show distribution of FeO*/MgO and TiO₂ in all Leg 54 basalts, our unpublished data from Leg 37, DSDP Leg 16 data from Yeats et al. (1973), and DSDP Leg 34 data from Bunch and La Borde (1976). The dashed boundary in the figure indicates the field of FAMOUS glasses as given by Bryan et al. (1976). The diagram reveals several interesting points: (1) There is broad covariation of all the data plotted, despite the samples being from different oceans, (2) The field of FAMOUS glasses encloses a significant portion of the plotted data, although the latter are distributed over a wide range of ages and environments in different oceans, (3) A fairly large number of Pacific analyses significantly exceed those from the Atlantic in both FeO*/MgO and TiO₂, (4) All EPR normal fabric basalts, SFZ, and GR Site 424 basalts plot in the direction of higher FeO*/MgO and higher TiO₂ and by and large outside the field of FAMOUS glasses, (5) The OCP moat basalts plot within the field of FAMOUS glasses with relatively large variation in FeO*/MgO as compared with TiO₂, and (6) Hole 425 basalts also plot within the field of FAMOUS glasses and show a proportional variation in FeO*/MgO and TiO₂.

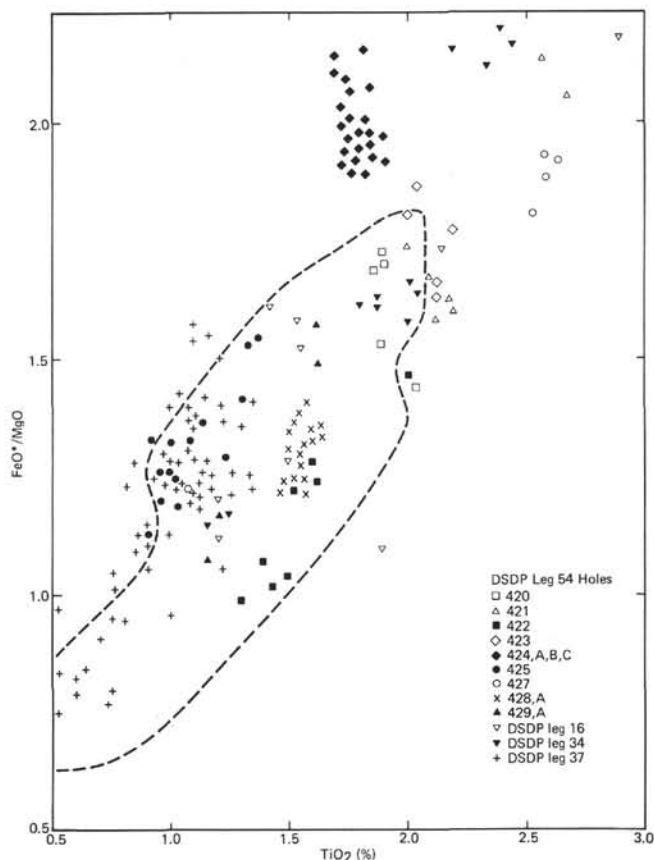


Figure 15. Covariation of FeO*/MgO and TiO₂ for Leg 54 basalts. DSDP Legs 16 and 34 data after Yeats et al. (1973) and Bunch and LaBorde (1976), respectively. Leg 37 data are our unpublished data. The dashed boundary encloses the field of FAMOUS glasses as given by Bryan et al. (1976).

In general, Leg 54 basalts are characterized by higher FeO and higher TiO₂ than Atlantic basalts. The higher FeO and higher TiO₂ may be related to the faster spreading rate in the Pacific. Melson et al. (1976) also show that the EPR and Juan de Fuca Ridge averages are characterized by distinctly higher FeO and TiO₂ than the Atlantic and Indian ocean averages.

P, Ti, Zr, and Y are generally enriched in alkali basalts relative to tholeiitic basalts. Most of the ocean-floor and ridge tholeiitic rocks have less than 1.8 per cent TiO₂ and less than 120 ppm Zr. Oceanic island tholeiites have higher Ti and Zr contents (Floyd and Winchester, 1975; Cann, 1970). All EPR normal fabric basalts and the SFZ basalts have more than 1.8 per cent TiO₂ and more than 150 ppm Zr. The OCP moat basalts have lower Ti and lower Zr, the range being similar to that of ocean-floor and ridge basalts. The GR basalts show a very wide range; as TiO₂ varies from 0.96 to 1.88 per cent, Zr varies from 46 to 130 ppm. The high degree of positive correlation between the pairs Ti-Zr and Ti-Y in the present tholeiites may either be attributed to the fact that these elements are strongly partitioned into residual liquid as crystallization proceeds (their partition coefficients into solid phases is nearly zero) and their absolute abundances are related to the degree of fractional crystallization which the melts have undergone, or else the positive correlation is a result of various degrees of partial melting of a homogeneous mantle. A more realistic approach is that the level of abundances of these elements as well as some others such as P and K in these basalts is related to both fractional crystallization and the degree of partial melting. Relatively high Zr contents of EPR normal fabric basalts and SFZ basalts may indicate a slight enrichment of Zr in the source of these rocks.

In Table 8 we show a comparison of EPR normal fabric basalts, OCP moat basalts, and the SFZ basalts with regard to their petrography, physical properties, and chemistry. Also listed are some literature data from the SFZ. The table clearly reveals that there are significant differences in petrography, physical properties, and chemistry of basalts from these sites. From the point of view of major oxide chemistry, the SFZ basalts are most evolved, having highest Fe, Ti, Zr, and FeO/MgO; the OCP moat basalts are least evolved, with lowest Fe, Ti, Zr, and FeO/MgO. The EPR normal fabric basalts have values intermediate between those of the SFZ and OCP moat basalts.

In the light of differences in the petrography and chemistry between the EPR normal fabric basalts and the OCP moat basalts, as discussed in the preceding paragraphs, it may well be that the latter basalts were not generated at the EPR proper but are related to later transform fault activity. The OCP ridge may mark the beginning of a new transform fault zone.

Despite having high Fe, Ti, P, and Zr, the SFZ basalts have extremely low K compared with EPR normal fabric basalts and EPR crest basalts from north and south of the fracture zone. This may indicate a different source composition for these basalts. Alternatively, this might be taken to indicate a higher degree of partial

melting of a similar large-ion-lithophile (LIL) element-depleted source, followed by extensive low-pressure fractional crystallization resulting in gradual enrichment of Fe and Ti. The high degree of iron enrichment (12.46% FeO) in these rocks requires some 70 to 80 per cent crystallization of a liquid of the composition of OCP moat basalt (the most primitive tholeiite recovered during Leg 54). Despite this, these residual liquids have retained the LREE-depleted patterns characteristic of normal ridge segments, although they have a much higher overall enrichment (almost double that of OCP moat basalts). This kind of REE enrichment is to be expected if the crystallization process is dominated by extraction of plagioclase and clinopyroxene with subordinate olivine. According to Clague and Bunch (1976), basalts, high in FeO, TiO₂, P₂O₅, K₂O, Na₂O, and SiO₂, and low in MgO, CaO, and Al₂O₃ (relative to normal mid-ocean ridge basalts) from the EPR, Galapagos, and Juan de Fuca Ridge are formed by fractionation of plagioclase, clinopyroxene, and olivine in average proportion of 9.3:7.1:1 from normal ridge tholeiites. Some 75 per cent of the original liquid has to crystallize to form ferrobasalts. Batiza et al. (1977) report that their most fractionated Siqueiros tholeiite (SD6-3, very similar to present SFZ basalts) can be derived from their primitive tholeiite SD8-3 (somewhat similar to OCP moat basalts) by fractionation and removal of 47 per cent plagioclase, 46 per cent clinopyroxene, and 7 per cent olivine. Removal of up to 80 weight per cent of crystals from such a liquid is therefore necessary.

The presence of highly fractionated tholeiites in transform fault troughs of the SFZ is contrary to the finding of Batiza et al. (1977), who report that highly fractionated tholeiites are absent in their dredge hauls from the northern and southern Siqueiros transform fault troughs. According to Crane (1976), the northern Siqueiros transform fault is the presently active transform fault, and the southern transform fault ceased to be active as strike slip motion and was taken up along the northern trough. Site 427 is certainly older than 1.2 m.y. (oldest sediments at the site), and so there is every likelihood that these basalts were produced at a time when the southern transform fault was still active.

Holes 423, 421, 420, and 429A form a nearly east-west transect on the west flank of the EPR with Hole 429A on the oldest crust. Thus, these holes offer an opportunity to study the composition of basalts in relation to their distance from the Rise crest. In Table 9, we list the average composition of basalts found at these sites as well as the analyses of other Rise crest basalts from the region. The table reveals that (1) among the EPR normal fabric basalts, Hole 429A tholeiites are the most primitive with regard to their Ti, Mg, alkalies, Zr, Ni, and FeO/MgO and S.I. values; the magma group of Core 421-1 (see analysis in Table 5a) seems to be the most evolved, having highest Ti, alkalies, Zr, and FeO/MgO, (2) in general it can be said that Ti, alkalies, Zr, and the ratio FeO/MgO show an increase toward the Rise crest, and Mg, Ni, and S.I. show a decrease. To a certain extent, Al and Ca also show an increase away from the Rise crest. However, the magma group of Core

TABLE 8
Comparison of EPR Normal Fabric Basalts, OCP Moat Basalts, and SFZ Basalts

	EPR Normal Fabric Basalts	OCP Moat Basalts	SFZ Basalts		
Petrographic description	Aphyric to sparsely phyric, glassy to fine- grained plagioclase- pyroxene basalts	Fine- to medium- grained olivine basalts	Fine- to medium-grained plagioclase-pyroxene basalts		
Physical properties ^a					
Velocity	5.2 to 5.7 km/s	5.8 to 6.2 km/s	5.7 km/s		
Density	2.8 to 2.88 g/cm ³	2.92 g/cm ³	2.92 g/cm ³		
Composition	Average of 20 analyses	Average of 25 analyses	Core 427-1 ^b	SD6-3 ^c	SD8-3 ^c
SiO ₂	50.65	50.20	50.05	48.00	50.30
TiO ₂	2.07	1.52	2.58	2.70	0.93
Al ₂ O ₃	13.71	14.78	13.79	12.80	15.60
FeO (total Fe)	10.89	9.70	12.46	13.66	8.59
MgO	6.57	7.72	6.60	5.98	9.80
CaO	10.69	11.52	9.77	10.14	12.77
Na ₂ O	2.61	2.62	2.97	3.33	2.41
K ₂ O	0.43	0.17	0.09	0.27	0.06
P ₂ O ₅	0.18	0.15	0.30	0.23	0.09
Ni	68	75	53	43	130
Y	43	26	45	—	—
Sr	120	140	121	140	125
Zr	163	103	191	—	—
La	—	4.14	6.93	—	—
Yb	—	2.95	4.90	—	—
FeO/MgO	1.66	1.27	1.89	2.29	0.88

^aData from the preliminary shipboard report.

^bAverage of four analyses from Hole 427.

^cSiqueiros fracture zone basalts from Batiza et al. (1977).

TABLE 9
Chemical Variation Away from the EPR Crest at 9° N

Sample Location	EPR Crest		Hole 423	Hole 421	Hole 420	Hole 429A
	SD5=1 ^a	SD5=2 ^a				
Age			1.6 m.y.	3.4 m.y.	3.4 m.y.	4.6 m.y.
SiO ₂	50.70	49.80	50.54	50.77	50.64	50.55
TiO ₂	2.26	1.64	2.11	2.27	1.93	1.62
Al ₂ O ₃	13.60	14.00	13.62	13.27	14.18	14.35
FeO (Total Fe)	12.70	10.59	11.37	11.37	10.68	11.07
MgO	6.94	8.16	6.44	6.43	6.64	7.18
Alkalies	3.84	3.81	3.11	3.14	2.96	2.79
Ni	43	—	53	67	82	88
Sr	185	—	126	123	115	115
Zr	—	—	161	185	161	103
FeO/MgO	1.83	1.30	1.77	1.77	1.61	1.54

^aFrom Batiza et al. (1977).

421-1 marks a reversal of the trend. Furthermore, there are significant differences in the analyses of two Rise crest samples from Batiza et al. (1977). Bonatti and Fisher (1971) also report large differences in Rise crest basalts from 10° S. Yeats et al. (1973) report, with respect to DSDP Leg 16 basalts, an increase in CaO and MgO and decrease in TiO₂, K₂O, and Na₂O with increasing distance from the crest of the EPR. Here also, the trends do not extrapolate to the Rise crest data.

Evidence for a crustal low-velocity zone below the EPR crest near the Siqueiros fracture zone has been presented by Orcutt et al. (1976) and Rosendahl et al. (1976). The latter have interpreted this zone as a shallow magma chamber below the EPR crest. The range of

chemical variation encountered within the EPR normal fabric basalts is certainly a result of shallow-level or, in other words, low-pressure fractional crystallization of the phase assemblage ol + pl + cpx, olivine being the least dominant of the three. This fractionation could take place either in the magma chamber below the EPR or in the conduit system that replenishes the chamber from below. The reversal of trends at Hole 421 in all probability marks the influx of new material to the magma chamber. Thus, a batch of magma undergoes shallow-level fractional crystallization in the low-velocity zone below the EPR. After some period, fresh material is added, depressing the differentiation indices of the existing liquid which, when subsequently erupted, gives rise to a more primitive basalt than that which erupted earlier.

Like the EPR basalts, the GR basalts are the product of low-pressure fractional crystallization of LIL-depleted melts. The degree of partial melting, however, was greater than that for EPR basalts. It is for this reason that the GR basalts are depleted in alkalies, Zr, and Sr in comparison with EPR basalts. The contention of Campsie et al. (1973) that the basalts from within the region of the large-amplitude magnetic anomaly are "plume-derived," indicating chemical similarity to Galapagos Island tholeiites, is not borne out by our results. On the other hand, our data support Anderson et al. (1975), who observed that Fe- and Ti-enriched basalts from the region of the large-amplitude magnetic anomaly cannot be formed by mixing of ridge tholeiite

and Galapagos Island tholeiite but are the result of extensive shallow-fractional crystallization of normal ridge tholeiite, producing Fe-enriched basalts which probably constitute one-third to one-half of Layer 2A.

ACKNOWLEDGMENTS

This work was done at the Institut für Petrographie und Geochemie, Universität Karlsruhe, Karlsruhe, West Germany, during RSK tenure as AvH Fellow in that Institute. The work was supported by a grant from the Deutsche Forschungsgemeinschaft. Neutron activation analyses were carried out with equipment given by Bundesministerium für Forschung und Technologie. Irradiation facilities were provided by the Gesellschaft für Kernforschung Karlsruhe. The help of U. Kramar in the INAA investigation is gratefully acknowledged. Last but by no means least, RKS is also grateful to the scientific party and crew members of the *Glomar Challenger* for their excellent cooperation during the 54th cruise.

REFERENCES

- Anderson, R. N., Clague, D. A., Klitgord, K. D., Marshall, M., and Nishimori, R. K., 1975. Magnetic and petrologic variation along the Galapagos spreading center and their relation to the Galapagos melting anomaly. *Bull. Geol. Soc. Am.*, v. 86, p. 683-694.
- Batiza, R., Rosendahl, B. R., and Fisher, R. L., 1977. Evolution of oceanic crust 3. Petrology and chemistry of basalts from East Pacific Rise and Siqueiros transform fault. *J. Geophys. Res.*, v. 82, p. 265-276.
- Bonatti, E., and Fisher, D. E., 1971. Oceanic basalts: chemistry versus distance from oceanic ridges. *Earth Planet. Sci. Lett.*, v. 11, p. 307-311.
- Bryan, W. B., Thompson, G., Frey, F. A., and Dickey, J. S., 1976. Inferred geologic settings and differentiation in basalts from the Deep Sea Drilling Project. *J. Geophys. Res.*, v. 81, p. 4285-4304.
- Bunch, T. E., and LaBorde, R., 1976. Mineralogy and composition of selected basalts from DSDP Leg 34. In Yeats, R. S., Hart, S. R., et al., *Initial Reports of the Deep Sea Drilling Project*, v. 36: Washington (U. S. Government Printing Office), p. 263-275.
- Campsie, J., Bailey, J. C., and Rasmussen, M., 1973. Chemistry of tholeiites from the Galapagos Island and adjacent ridge. *Nature Phys. Sci.*, v. 245, p. 122-124.
- Cann, J. R., 1970. Rb, Sr, Y, Zr and Nb in some ocean floor basaltic rocks. *Earth Planet. Sci. Lett.*, v. 10, p. 7-11.
- , 1971. Major element variation in ocean floor basalts. *Phil. Trans. Roy. Soc. London*, v. 268, p. 494-505.
- Chayes, F., 1965. The silica-alkali balance of basalts of submarine ridges. *Carnegie Inst. Wash. Yr. book*, v. 64, p. 155-163.
- , 1966. Alkaline and subalkaline basalts. *Amer. J. Sci.*, v. 264, p. 128.
- Clague, D. A., and Bunch, T. E., 1976. Formation of ferrobasalts at East Pacific midocean spreading centers. *J. Geophys. Res.*, v. 81, p. 4247-4256.
- Coombs, D. S., 1963. Trends and affinities of basaltic magmas and pyroxenes as illustrated on diopside-olivine-silica diagram. *Mineral. Soc. Am. Special Paper 1*, p. 227-250.
- Crane, K., 1976. The intersection of Siqueiros transform fault and the East Pacific Rise. *Mar. Geol.*, v. 21, p. 25-46.
- Engel, A. E., Engel, C. G., and Havens, R. G., 1965. Chemical characteristics of oceanic basalts and upper mantle. *Bull. Geol. Soc. Am.*, v. 76, p. 719-734.
- Flanagan, F. J., 1973. 1972 values for international geochemical standards. *Geochim. Cosmochim. Acta.*, v. 37, p. 1189-1200.
- Floyd, P. A. and Winchester, J. A., 1975. Magma type and tectonic setting discrimination using immobile elements. *Earth Planet. Sci. Lett.*, v. 27, p. 211-218.
- Green, D. H. and Ringwood, A. E., 1967. The genesis of basaltic magmas. *Contrib. Mineral. Petrol.*, v. 15, p. 103.
- Kay, R., Hubbard, N. J., and Gast, P. W., 1970. Chemical characteristics and origin of ocean ridge volcanic rocks. *J. Geophys. Res.*, v. 75, p. 1585-1613.
- Kempe, D. R. C., 1975. Normative mineralogy and differentiation patterns of some drilled and dredged oceanic basalts. *Contrib. Mineral. Petrol.*, v. 50, p. 305-320.
- Kuno, H., 1968. Differentiation of basaltic magmas. In Hess, H. H., and Poldervaart, A., (Eds.). *Basalt: The Poldervaart Treatise on Rocks of Basaltic Composition*, v. 2: New York (Interscience).
- Macdonald, G. A. and Katsura, T., 1964. Chemical composition of Hawaiian lavas. *J. Petrol.*, v. 5, p. 82-133.
- Melson, W. G., Vallier, T. L., Wright, T. L., Byerly, G., and Nelen, J., 1976. Chemical diversity of abyssal volcanic glass erupted along Pacific, Atlantic and Indian ocean sea floor spreading centres. *The Geophysics of the Pacific Ocean Basin*, Geophysical Monograph Series, v. 19, Washington (American Geophysical Union).
- Miyashiro, A., 1975. Classification, characteristics and origin of ophiolites. *J. Geol.*, v. 83, p. 249.
- Miyashiro, A., Shido, F., Ewing, M., 1969. Diversity and origin of abyssal tholeiite from Mid-Atlantic Ridge near 24° and 30° N latitude. *Contrib. Mineral. Petrol.*, v. 23, p. 38-52.
- Nicholls, G. D., 1965. Basalts from the deep-ocean floor. *Mineral. Mag.*, v. 34, p. 373.
- Orcutt, J. A., Kennett, B. L. N., and Dorman, L. M., 1976. Structure of East Pacific Rise from an ocean bottom seismometer survey. *Geophys. J. Roy. Astron. Soc.*, v. 45, p. 305-320.
- Pearce, J. A., 1975. Basalt geochemistry used to investigate past environment on Cyprus. *Tectonophysics*, v. 25, p. 41-67.
- Pearce, J. A., and Cann, J. R., 1971. Ophiolite origin investigated by discriminant analysis using Ti, Zr, and Y. *Earth Planet. Sci. Lett.*, v. 12, p. 339-349.
- , 1973. Tectonic setting of basic volcanic rocks determined using trace element analyses. *Ibid.*, v. 19, p. 290-300.
- Puchelt, H., and Kramar, U., 1974. Standardization in neutron activation analysis of geochemical material. Working paper presented at IAEA Panel Meeting on Nuclear Geophysics and Geochemistry, 25-29 November 1974, Vienna.
- Rosendahl, B. R., 1976. Evolution of oceanic crust 2. Constraints, implications and inferences. *J. Geophys. Res.*, v. 81, p. 5305-5314.
- Rosendahl, B. R., Raitt, R. W., Dorman, L. M., Bibee, L. D., Hussong, D. M., and Sutton, G. H., 1976. Evolution of oceanic crust 1. A physical model of the East Pacific Rise Crest derived from seismic refraction data. *Ibid.*, v. 94, p. 5294-5304.
- Scheidegger, K. F., 1973. Temperature and composition of magmas ascending along midocean ridges. *Ibid.*, v. 78, p. 3340-3355.
- Schilling, J. G., 1971. Sea-floor evolution: rare earth evidence. *Phil. Trans. Roy. Soc. London A*, v. 268, p. 663-706.
- Schilling, J. G., 1975. Rare earth variations across normal segments of Reykjanes ridge, 60°-53° N, mid-Atlantic ridge, 29° S and East Pacific rise 2°-19° S, and evidence on composition of the underlying low-velocity layer. *J. Geophys. Res.*, v. 80, p. 1459-1473.
- Schilling, J. G., Anderson, R. N., and Vogt, P., 1976. Rare earth, Fe and Ti variations along the Galapagos spreading

- centre, and their relationship to the Galapagos mantle plume. *Nature*, v. 261, p. 108-113.
- Shido, F., Miyashiro, A., and Ewing, M., 1971. Crystallization of abyssal tholeiites. *Contrib. Mineral. Petrol.*, v. 31, p. 251-266.
- Smith, R. E., and Smith, S. E., 1976. Comments on the use of Ti, Zr, Y, Sr, K, P, and Nb in classification of basaltic magmas. *Earth Planet. Sci. Lett.*, v. 32, p. 114-120.
- Srivastava, R. K., 1977. A comprehensive atomic absorption and spectrophotometric scheme for the determination of major and trace elements in rocks and minerals. *N. Jb. Miner. Mh. Year 1977*, p. 425-432.
- Williams, D. L., von Herzen, R. P., Sclater, J. G., and Anderson, R. N., 1974. The Galapagos Spreading Centre: Lithospheric cooling and hydrothermal circulation. *Geophys. J. Roy. Astron. Soc.*, v. 38, p. 587-ff.
- Yeats, R. S., Forbes, W. C., Heath, G. R., and Schiedegger, K., 1973. Petrology and geochemistry of Leg 16 basalts, eastern equatorial Pacific. In van Andel, Tj. H., Heath, G. R., et al. *Initial Reports of the Deep Sea Drilling Project*, v. 16: Washington (U. S. Government Printing Office), p. 617-640.

APPENDIX

Hole 420

Five samples of basalts from Cores 13, 14, 15, and 17, are included in this study. They are hyalocrystalline and dominated by glass components. All the samples are finely vesicular; some of the vesicles are filled with smectites.

In thin sections, the basalts show various degrees of crystallinity. Their texture ranges from glassy-spherulitic to intersertal. They are made up of plagioclase, clinopyroxene, and an occasional grain or two of olivine besides glass. Among the opaque minerals, titanomagnetite is by far the most abundant and may constitute 2 to 3 per cent of the rocks. On the basis of petrography, these basalts may be considered to be aphyric plagioclase-pyroxene basalts or simply aphyric basalts.

Hole 421

Seven samples of basalts from this hole fall broadly into two petrographic types, namely glassy basalts and aphyric to sparsely microphyric basalts. While the first type is found in Core 2 and in the upper part of Core 3, the second type constitutes the greater part of Cores 3 and 4 and the sample recovered in the bit. The main petrographic features of the two types are as follows:

1) Glassy basalts:

These are glassy rocks — glass constitutes 85 per cent of these rocks — with about 10 per cent variolitic patches and 2 to 3 per cent plagioclase and pyroxene microphenocrysts besides minor iron oxide minerals. The variolites are arborescent intergrowths of plagioclase and clinopyroxene. In places, there are sheaf-like varioles of pyroxenes. The glass present is light to dark brown in color and shows evidence of devitrification.

2) Aphyric to sparsely microphyric basalts:

These are fine-grained basalts with 1 to 2 per cent microphenocrysts of plagioclase and/or clinopyroxene. The unit differs from type 1 by lower glass content (less than 20 vol. %), larger microphenocrysts, and smaller amount of iron oxide minerals. The texture of these rocks is variolitic and intersertal.

Hole 422

Nine samples of basalts from this hole located in the northern moat of the OCP Ridge (Figure 1) are included in this study. Megascopically, these basalts can be grouped into two major groups: (1) light colored, fine- to medium-grained basalts, and (2) dark colored, almost glassy basalts, similar to the basalts from Holes 420 and 421. The shipboard scientific party termed the former "doleritic rock," and the latter "glassy basalt." For the sake of convenience, we have adopted the same terminology in describing these rocks.

1) Doleritic rocks:

There are two doleritic units at Hole 422 which are separated by about 4.0 meters of sediments (the term doleritic has been used for

a relatively coarse grained rock that may or may not be an intrusive). Texturally, these rocks are broadly similar; that is, most of them show intersertal to ophitic texture. The fine-grained rocks in general show intersertal texture, whereas the medium-grained ones are strongly ophitic. Mineralogically, they are essentially made up of plagioclase, clinopyroxene, and patches of glass (normally not exceeding 10 vol. % of the rocks). Besides these components, they contain a few grains of olivine. The amount of olivine in the samples from the lower part of Core 9 is relatively higher than that in the samples from Cores 7, 8, and the upper part of Core 9. Among the opaques, titanomagnetite is most common. Occasional sulfide blebs are also seen in these rocks.

2) Glassy basalt:

This type underlies the lower doleritic unit and consists of an aphyric glassy basalt which is texturally and mineralogically distinct from the overlying doleritic unit. The glassy groundmass, which is practically opaque, contains scattered thin, lath-like microphenocrysts of plagioclase and a few hourglass-zoned grains of clinopyroxene.

Hole 423

Five samples of basalts from Cores 5, 6, 7, and 8 are included in this study; these are essentially fine-grained to glassy, aphyric plagioclase-pyroxene basalts. They exhibit various textures like variolitic, hyalopilitic, and pilotaxitic. There are occasional microphenocrysts of plagioclase and clinopyroxene in these rocks. A great degree of textural and mineralogical similarity exists between these rocks and those from Holes 420, 421, and glassy basalts from Hole 422. The occurrence of chilled margins in many of the samples indicates the extrusive nature of these basalts.

Holes 428 and 428A

Drilled 500 feet apart south of the OCP Ridge, in an area marking the transition from the normal fabric to transverse ridge structure, the holes contain two types of basalts: (1) cryptocrystalline to fine-grained, aphyric olivine-bearing basalts, (2) fine- to medium-grained mesocratic doleritic rocks similar to the doleritic rock from Hole 422 (shipboard scientific party). While the former is found in Hole 428, and in the upper part (up to 15.5 m depth) of Hole 428A, the latter is confined to the lower part of Hole 428A. Seventeen samples from both these holes are included in the present study. Chief petrographic features of the two types of basalts are as follows:

1) Aphyric olivine basalts:

As the name suggests, these are aphyric, cryptocrystalline to fine-grained basalts occurring in Hole 428 and the upper part of Hole 428A. Microscopically, they are vesicular basalts with hyalopilitic to variolitic to intersertal and subophitic textures. The glassy portion in these rocks often shows sheaf-like varioles of incipient crystals of pyroxenes and plagioclase. In some sections, speckled brown glass is seen. Some of these rocks contain a few microphenocrysts of plagioclase and/or glomerocrysts of plagioclase and olivine. The amount of olivine is variable in these rocks, but never constitutes more than 1 to 2 per cent. Titanomagnetite is the common iron oxide mineral, accounting for 5 to 8 per cent.

2) Doleritic rocks:

As mentioned earlier, these rocks are found below 19.5 meters depth in Hole 428A. The top part of the unit immediately below the olivine basalts in Core 3 is a fine-grained aphyric type showing variolitic to intersertal texture. The mineralogical composition is plagioclase, clinopyroxene, and iron oxide minerals, which occur as subhedral to euhedral crystals. The rock is free from olivine. The grain size increases downhole and the texture changes from subophitic to ophitic.

Plagioclase in these rocks is lath-shaped, and generally well-twinned. Their composition is close to that of labradorite. Clinopyroxene is augite; it occurs as plates or large crystals (1.0 to 1.4 mm) enclosing plagioclase laths. The mineral sometimes shows twinning. In the lower part of the section, especially in Cores 6 and 7, one or two grains of olivine are seen. Titanomagnetite occurs as moderate- to large-sized, subhedral to euhedral crystals indicating a slow rate of cooling for these rocks. Their degree of alteration is limited.

Hole 429A

This is the oldest EPR site drilled during Leg 54, and its inferred magnetic anomaly age is 4.6 m.y. In general, the basalts from this hole

are fine-grained aphyric. Many of the samples, particularly from the upper part of Core 2, display chilled margins and have glassy edges. On the basis of thin section studies, the basalts from this hole can be grouped into two petrographic types: (1) aphyric olivine basalt, and (2) aphyric basalt. The former is confined to Core 1 and the upper part of Core 2; the latter is found in the lower part of the hole. Here it may be worthwhile to recall that rocks in the lower part of the hole have negative polarity, which agrees with the associated magnetic anomaly; in the upper part, however, the rocks show a positive polarity and are therefore almost certainly of younger age (see shipboard report).

1) Aphyric olivine basalts:

These are very fine grained basalts, showing hyalopilitic to variolitic texture. They contain some microphenocrysts of olivine and plagioclase. In the hyalopilitic varieties, the groundmass consists of skeletal plagioclase laths and extremely fine sheaves of clinopyroxenes in a matrix of devitrified glass. In the more crystalline varieties it consists of almost equigranular plagioclase, clinopyroxene, and irregular patches of glass. The titanomagnetite grains are skeletal and their size varies from 10 to 15 μm .

2) Aphyric basalts:

These rocks differ from the earlier types in their grain size, being relatively coarser grained, and in their being devoid of olivine grains. The amount of glass in these rocks is also much less than in type-1 basalts. Petrographically, they look similar to the basalts from Holes 420 and 421.

Hole 427 (SFZ)

Four samples of basalts from this hole are included in this study. Megascopically, these are fine- to medium-grained, mesocratic basalts with a relatively large number of vesicles commonly filled in with smectites. Microscopically, these are almost holocrystalline basalts showing subophitic to intergranular texture. The chief mineral constituents are plagioclase, clinopyroxenes, and minor amounts of titanomagnetite. Occasional phenocrysts of plagioclase and clinopyroxene are also seen in these rocks.

Holes 424A, B, and C (GR)

Twenty-four samples of basalts from four holes drilled in the "Mounds Hydrothermal Field" close to the ridge crest of the GR are included in this study. The magnetic anomaly age of this site is 0.69 m.y., and as such it is the youngest site drilled. Megascopically, the basalts recovered from these holes are very similar and are fine- to medium-grained, vesicular aphyric basalts with occasional microphenocrysts of plagioclase. Microscopically, these basalts show different textures; the samples that are quenched show intersertal and variolitic textures, whereas relatively coarser samples (fine- to medium-grained) show intergranular texture. Mineralogically, these are made up of plagioclase, clinopyroxene, and variable amounts of glass and titanomagnetite. The content of titanomagnetite in these rocks is approximately 10 per cent, and the glass content varies from 10 to 35 per cent. Even the relatively coarser grained samples are not devoid of glass but contain glassy segregations which contain needlelike opaques, dendritic clinopyroxene, and sometimes microphenocrysts of plagioclase. In general, the petrographic studies reveal that there are no different petrographic types in these holes, and the textural variations represent different cooling units.

Hole 425

Fourteen samples of basalts from this hole are included in this study. Megascopically, these basalts show large variations in their color, grain size, nature of vesiculation, and in the phenocryst assemblages both as to their size and nature (that is, they occur as either single crystals or glomerocrysts, or both). In general they can be termed fine- to medium-grained, aphyric to phyric basalts without any significant alteration.

On the basis of the thin section studies, basalts from this site can be grouped into five petrographic types, two of which may not be distinct types. Furthermore, these types repeat themselves throughout each hole. The description of the various types is as follows:

1) Fine-grained aphyric basalts:

These occur in the upper part of Core 7 and in the middle of Core 9; they are fine-grained, vesicular basalts with intersertal to variolitic texture. Some of the thin sections, especially those from Core 9, show pilotaxitic texture. As regards the mineralogical com-

position, this is essentially made up of plagioclase, clinopyroxene, iron oxide minerals, and glass. In some thin sections, there are suspect grains of olivine. Plagioclase is commonly lath-shaped labradorite. Clinopyroxenes in these rocks are brownish to pinkish in color; they occur as subequant grains or needlelike crystals showing a fan-shaped arrangement, indicating sudden chilling. The iron oxide minerals are mostly titanomagnetite and occur as dissemination or skeletal crystals, which again suggests rapid cooling of these rocks. The glassy material within the rocks occurs as dark colored disseminated patches. The vesicles present are mostly filled with smectite.

2) Pyroxene-plagioclase sparsely phyric basalts:

Like the petrographic type 1, these basalts also repeat in the hole; that is, they are found below the type-1 basalts in Core 7 and in the middle of Core 8. As compared with the type-1 basalts, these are much coarser in grain size and have occasional phenocrysts or microphenocrysts of both plagioclase and clinopyroxene. The amount of iron oxide minerals and glass present in these rocks is also much lower than in the type-1 basalts. It is not unlikely that the type-1 basalts represent the chilled portions of these basalts.

3) Phyric-glomeroporphyritic basalts:

These are the most abundant type of basalt found at this hole and constitute almost one-third of the total section. They make up a thick unit in Cores 7 and 8, and a thin unit at the top of Core 9. These are essentially fine- to medium-grained, almost holocrystalline porphyritic to glomeroporphyritic rocks with minor quantities of glass being confined to interstices in the groundmass.

The phenocrysts in these rocks comprise 5 to 8 volume per cent, and they occur both as individual crystals and glomerocrysts. The latter are made up either of plagioclase or of both plagioclase and pyroxene. The individual plagioclase phenocrysts range from 0.5 to 1.5 mm in size. The clinopyroxenes are between 0.5 and 1 mm in size. The plagioclase phenocrysts may show zoning and sodic overgrowths. Some of the clinopyroxene phenocrysts show wavy extinction, such that an extinction band sweeps across the grain.

The groundmass of these rocks is made up of plagioclase and clinopyroxene, with minor amounts of iron oxide minerals; and its texture varies from intergranular, intersertal, to variolitic. Occasionally, the groundmass pyroxenes are needle-shaped and show fan-shaped texture. The iron oxide minerals occur as skeletal crystals (only occasionally do they show subequant form), indicating a moderate to rapid cooling rate for these rocks. The presence of zoning, glassy inclusions, sodic overgrowths in plagioclase crystals, and wavy extinction of some clinopyroxene phenocrysts also point to rather rapid cooling. The metastable textural features indicate that the rocks are from flows rather than sills in which such metastable textures would have been annealed.

These rocks also show some evidence of post-crystallization deformation as shattering of grains and bending of plagioclase phenocrysts.

4) Glomeroporphyritic \pm olivine basalts:

This petrographic type is found in the lower part of Core 8, and it occurs between the petrographic type 2 above and petrographic type 3 below. There are some essential differences between this type and type 3, which are both in the nature and the sizes of phenocrysts as well as in the groundmass texture. The glomerocrysts of plagioclase, clinopyroxene, and olivine (rare) account for about 15 volume per cent of the rocks. The individual phenocrysts of plagioclase are sometimes as large as 3 to 4 mm in size; they are tabular in habit and appear to be more calcic than the phenocrysts in type 3. The olivine phenocrysts, when present, are up to 1.5 mm in size, and show alteration to smectites along cracks.

The groundmass of these rocks is much finer than that of the type-3 rocks and is made up of needlelike grains of pyroxene, thin laths of plagioclase, and glass. The iron oxide minerals are skeletal titanomagnetites. The nature of the groundmass and titanomagnetite suggests a rapid cooling rate for the unit after eruption. The glomerocrysts are most likely of pre-eruption crystallization origin, when the magma composition was still on the olivine-plagioclase-pyroxene cotectic.

5) Pyroxene-plagioclase \pm olivine sparsely phyric basalts:

This type is found at the bottom of the hole in Core 9; it is essentially similar to type 2, except that there are occasional grains of olivine in the groundmass as well as microphenocrysts. In hand specimens, the rock has a bleached appearance. The amount of iron oxide minerals is lower than that in type 2.